①

⑥

THE CONTINUOUS CRYSTALLIZATION OF ALUMINUM POTASSIUM SULPHATE IN AN AGITATED VESSEL.

⑨ Master's thesis,

A Thesis
Presented to
the Faculty of the School of Engineering and Applied Science
University of Virginia

⑫ 94 p.

In Partial Fulfillment
of the Requirements for the Degree
Master of Science (Chemical Engineering)

by

⑩ Richard D. Nidel, Sr.

⑪ Aug[illegible] 1977

401 975

APPROVAL SHEET

This thesis is submitted in partial fulfillment of the
requirements for the degree of
Master of Science (Chemical Engineering)

Author

This thesis has been read and approved by the Examining Committee:

Thesis Adviser

Accepted for the School of Engineering and Applied Science:

Dean, School of Engineering and
Applied Science

August, 1977

ABSTRACT

A continuous flow, mixed-suspension, mixed-product-removal crystallizer was constructed. The apparatus was shown to satisfy the assumptions necessary for the calculation of crystal growth velocities from the steady-state distributions of crystal sizes produced under various operating conditions. Although the growth velocities were of the same order-of-magnitude as those observed in single crystal studies, the crystallization kinetics obtained for the growth of potassium alum in this suspension crystallizer differed.

Solution trapping due to occlusion formation during crystal growth was also investigated. Previous workers have found signficant amounts of trapped solvent at various growth velocities in single crystals grown in flow crystallizers. Although some of these same growth velocities were attained in this study, no conclusive evidence of solution trapping was noted in the crystals grown in the suspension crystallizer. Several reasons for this discrepancy are also postulated.

ACKNOWLEDGEMENTS

The author would like to sincerely thank the following for their contributions to the successful completion of this work:

The United States Army for providing me with the opportunity to participate in this program;

My fellow students for their technical advice and friendship which they freely and abundantly extended.

Mr. Ed Elder for the patience and assistance he rendered during the construction of many of the components of the experimental apparatus.

Dr. J. L. Gainer for his confidence and friendship during the last 2 years.

Dr. D. J. Kirwan for his confidence, ideas, patience, understanding, wisdom, and time which he gave freely doing all aspects of this work. Little of this work could have been successfully completed without his guidance.

A special acknowledgement of love and gratitude are extended to my wife, Paulette, and my sons, Ricky and Chris. Without their support, prayers, and specialness, none of this work could have been completed.

TABLE OF CONTENTS

LIST OF FIGURES

LIST OF TABLES

NOMENCLATURE

A_1, A_2 - constants in Equation (5)

C_b - bulk liquid composition, where noted

C_L - composition of liquid

$C_L(o)$ - composition of liquid at interface

$C_L^*(o)$ - equilibrium composition of liquid

$C_L(\infty)$ - composition of bulk liquid where indicated

C_p - specific heat of liquid

C_s - composition of solid

D, D_V - diffusivity of impurity

G - imposed temperature gradient at the interface

h - height of a growing crystal layer

H_f - heat of fusion

I_W - mass of trapped water in Equation (26)

k_a - apparent distribution coefficient

k_a - crystal surface area shape factor, where indicated

k_e - effective distribution coefficient

k_m - mass transfer coefficient

k_o - equilibrium distribution coefficient

k_s - concentration of impurity in the surface layer divided by the concentration in the melt

k_V - crystal volumetric shape factor

K_V - constant in kinetic growth expression

K_1, K_2 - constants in Equation (6)

L - linear dimension of a crystal (diameter)

$\bar{L}$ - average crystal size based on 2 successive screen sizes

L^* - smallest measureable diameter, 75 μm

m - slope of the liquidous line on the phase diagram

M - mass of crystal on a given screen

M_T - concentration of suspended solids on a per liter slurry basis

n - temperature dependence of kinetic growth expression in Equation (6)

n - population density function

n^* - population density at size $L^* = 75$ μm

N - number of crystals in a size range

Q - volumetric flow rate

v - crystallizer volume

V - crystal linear growth velocity

W - mass fraction of crystal in a size range

W_b - weight of baked crystal residue

W_c - weight of crystal

X_{H_2O} - mass ratio of water to anhydrous alum in Equation (26)

α - thermal diffusivity

ρ - mass density

τ - residence time

CHAPTER I

INTRODUCTION

Crystallization is an age-old, commonly used purification or separation process. This process is widely used industrially with applications ranging from the preparation of "freeze-dried" foods, fruit juice concentrates, the production of chemical reagents and pharmaceuticals, to the purification of semiconductor materials.

While the practice of crystallization has been in use since before the days of the alchemists, its theoretical developments, particularly with application to industrial processes, have been limited. Few satisfactory theories exist to adequately describe how crystal nuclei form and how these nuclei ultimately grow. Because of this limited theoretical base, crystallization in general, and industrial-scale crystallization in particular, remain more an art than a science.

The two most widely used crystallization techniques are crystallization from the melt, and crystallization from solution. Crystallization from the melt generally is the crystallization of the component that is present in the largest quantity in the liquid phase, i.e. the solvent. Crystallization from the melt, via the zone refining technique, has produced ultrapure crystalline materials used as semiconductors. Crystallization from solution, on the other hand, freezes the solute out of solution. This is the most commonly used of the two techniques, and the crystallizing apparatus may range from a simple batch operation with natural cooling, to complicated continuous cooling crystallizers, or to vacuum crystallizers which cool and supersaturate by the evaporation of the solvent.

Regardless of the technique employed, the purpose of a crystallization process is to facilitate the mechanical separation of the solvent and solute upon the freezing of either of these constituents. The equilibrium relationship between crystal and the concentration of the solution from which it is formed can be obtained from a solubility or phase diagram. The use of the solubility diagram in crystallization is analogous to the use of boiling point diagrams in distillation. The concentration of the solute in a saturated solution, at equilibrium with solid, may be obtained at a given temperature.

Until recently, the solubility diagram for an eutectic system, one exhibiting no solid-solid solubility, was thought sufficient to predict the extent of separation which could be effected by a decrease in temperature. However, it has been often observed that less separation than predicted theoretically, from the equilibrium phase diagram, can be achieved experimentally.

It has been shown that under conditions where a planar crystalline interface becomes unstable, the crystal may grow in a "spiked" fashion. These spikes or dendrites may grow in three dimensions to entrap pockets or occlusions of solution. The formation of occlusions and the resultant trapping of solvent has been experimentally studied and correlated by Edie[1] in crystallization from the melt, and by Myerson[2] during crystallization from solution. Myerson[2] has also developed and tested a correlation, based upon a computer simulation of dendritic growth, which predicts the extent of solvent trapping for given growth conditions. He confirmed the usefulness of the correlation for both melt growth and for the growth of single crystals from solution in a flow crystallizer.

The majority of applications of industrial crystallization from solution are conducted in agitated vessels, usually operated continuously. In such systems crystallization occurs in a suspension containing a large number of crystals, in which both nucleation and growth are occurring. It is the purpose of this work to design and to build a laboratory, continuous, cooling crystallizer, similar to most industrial scale operations, and to investigate the occurrence of solution trapping by occlusion formation under kinetic conditions similar to those of Myerson in his single crystal studies. If this phenomenon occurs, the applicability of Myerson's correlation for a flow crystallizer will be ascertained for a continuous, suspension crystallization process.

CHAPTER II

LITERATURE SURVEY AND THEORETICAL BACKGROUND

The process of crystallization involves a phase change from liquid to solid in which the equilibrium compositions of the two phases at a given temperature generally differ. These conditions are most readily described on a phase diagram or solubility diagram. Many binary systems have eutectic phase diagrams, ones in which there is no solid-solid solubility. As a result, a pure component crystal should be produced upon the cooling of the binary solution. Such a eutectic phase diagram is shown in Figure 1 for the system salol-thymol. In contrast, the phase diagram of a system exhibiting solid-solid solubility is shown in Figure 2. Figure 2 is seen as comparable to the liquid-vapor phase diagram of two miscible liquids as seen in Figure 3 for the system benzene-toluene.

The ratio of the solid to liquid composition from the phase diagram is referred to as the equilibrium distribution coefficient, k_o, defined by

$$k_o = \frac{C_S}{C_L(o)} \qquad (1)$$

where

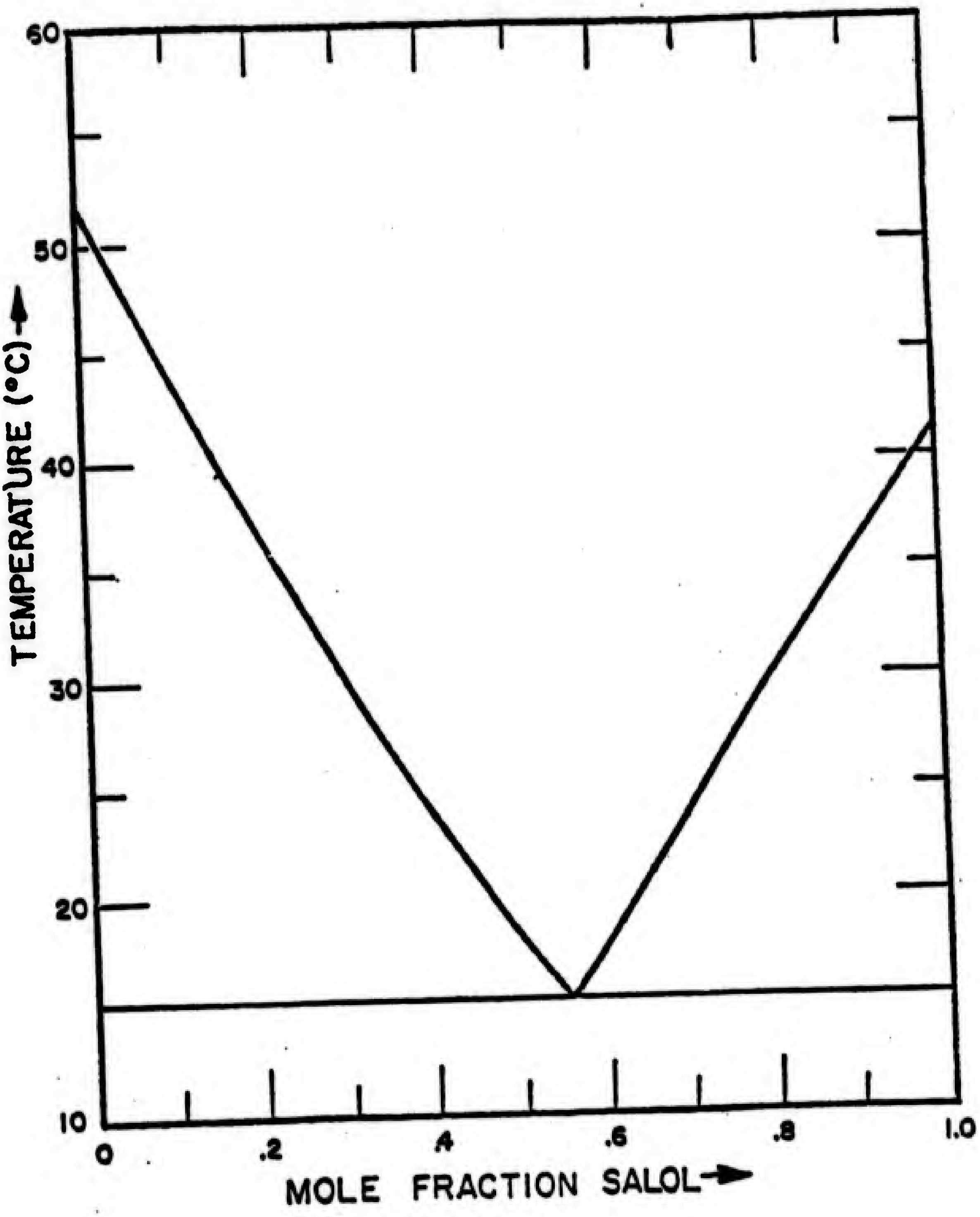

Figure 1. Phase diagram for a eutectic system.

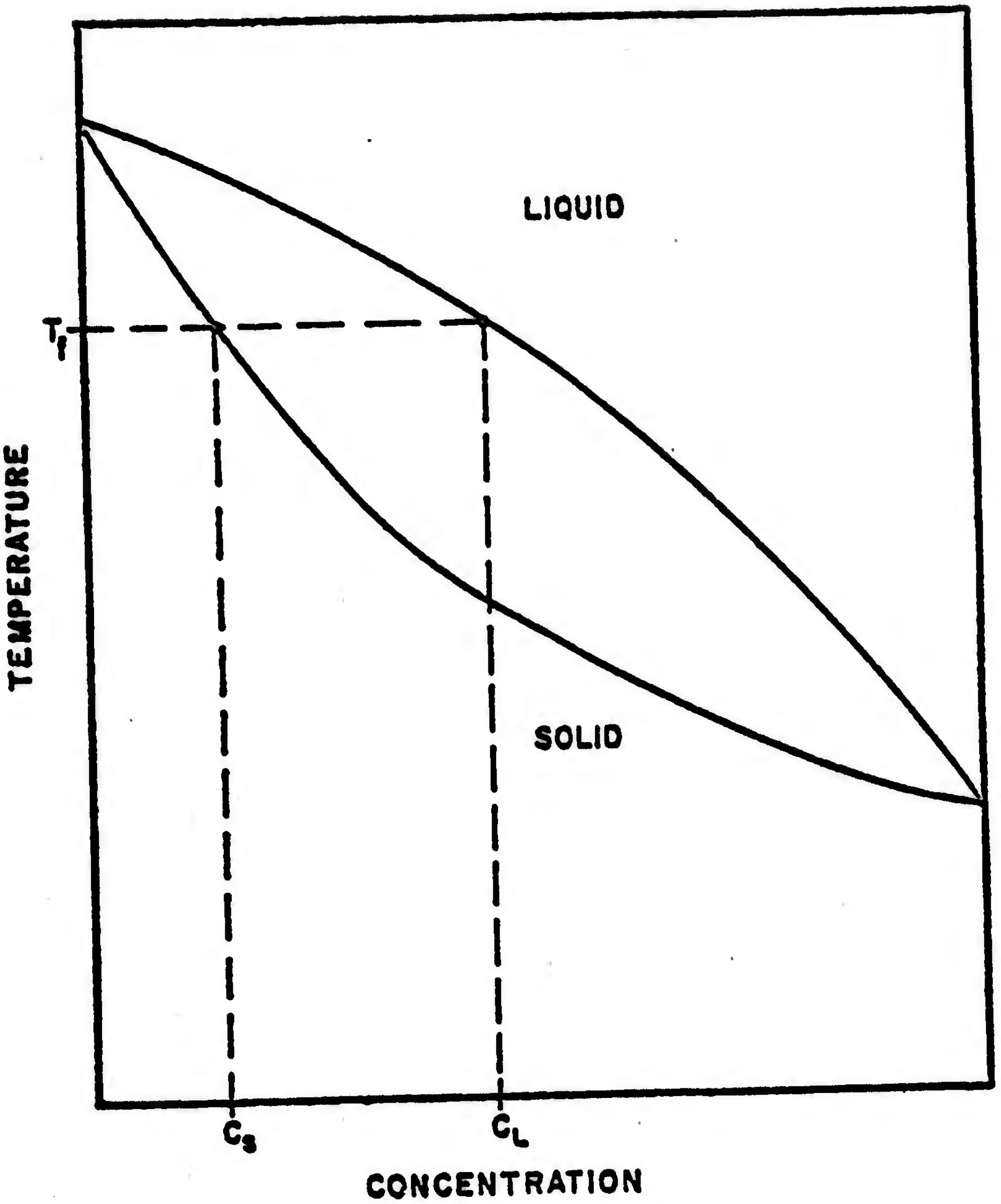

Figure 2. Phase diagram for a system with solid-solid solubility.

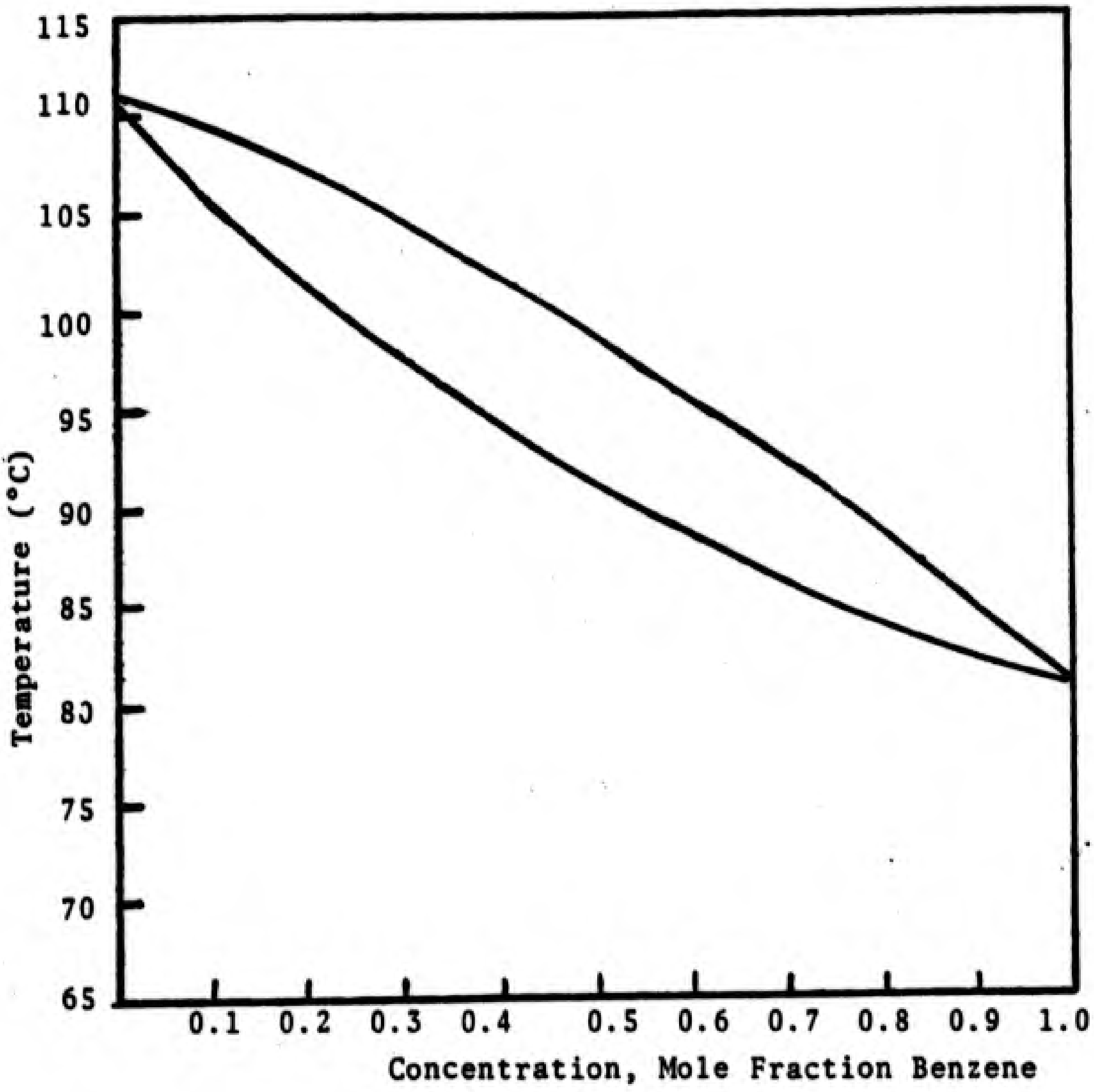

Figure 3. Vapor-liquid phase diagram for the system benzene-toulene at 1 atm.

C_S = composition of the solid (grams/liter)
C_L = composition of the liquid (grams/liter)

Crystals grown at low growth velocities such as those normally experienced under laboratory conditions, usually exhibit the compositions predicted by the equilibrium phase diagram. Industrial crystallization processes, however, often require much higher growth velocities in order to meet production and/or cost requirements. From experiments at these higher growth rates, it has been seen that non-equilibrium compositions of the components were present. Many investigators of crystalline impurities have reported inclusions in the crystalline structure. Brooks, Horton, and Torgeson,[3] Denbigh and White[4] and others mentioned in a review by Wilcox[5] have observed impurities trapped in crystals grown from solution. Edie and Kirwan,[6] Cheng and Pigford,[7] Kirwan and Pigford,[8] Janzow and Chao[9] and Ozüm and Kirwan[10] have studied this phenomenon in various melt systems. The result of this trapping is a non-equilibrium distribution of components and hence, crystal impurity. In systems which demonstrate solid-solid solubility, an <u>excess</u> amount of the component whose composition in the solid decreases upon freezing has been observed. The term impurity has been used to describe the presence of a component whose existence is not justified by the equilibrium phase diagram. This term will be frequently used throughout this discussion.

In an effort to account for the presence of non-equilibrium compositions, early investigators of solid-liquid separation defined an "effective" distribution coefficient

$$k_e = \frac{C_S}{C_L(\infty)} \qquad (2)$$

which is based on the concentration of the solid and the bulk liquid concentration. While this relationship aids the correlation of data, it does not attempt to account for any discrepancies at the solid-liquid interface. This problem arises mainly from the difficulty in determining the actual solid-liquid compositions at the interface.

As noted above, numerous investigators have observed the incorporation of impurities in crystals grown both in solution and from the melt. Some of the theories which have been proposed to explain this phenomenon will next be reviewed. Then a discussion of the theory of continuous suspension crystallizers will be presented to demonstrate how occlusion formation in such systems can be studied and correlated.

A. Experimental Observations and Theories of Impurity Capture

One of the first explanations of impurity trapping came in a theory proposed by Chernov[11] and Hall.[12] The theory proposed that molecules of the impurity are adsorbed onto the surface of a growing crystal. They viewed the crystallization process as a motion of steps of height h across the crystal surface, and postulated that, if the crystal growth velocity normal to the surface is greater than D/h (where D is the diffusivity of the impurity), the adsorbed impurity will be covered by the growing crystal layer, and consequently trapped. Hall[12] then developed a new effective distribution coefficient which related the amount of trapped impurity to its concentration in the melt, its equilibrium value, its diffusivity, and the crystal growth velocity

$$k_e = k_o + (k_s - k_o)\exp -(\frac{D/h}{V}) \qquad (3)$$

where

k_s = concentration of impurity in the surface layer divided by concentration in the melt ($= C_L(o)/C_L(\infty)$)

k_o = equilibrium distribution coefficient

V = growth velocity normal to the surface

This theory worked well in accounting for small amounts of impurities found in semi-conductor material, such as silicon and germanium. Botsaris <u>et al</u>.[13] used this theory to investigate the incorporation of P_b^{++} ions during the growth of KCl crystals from solution. They reported large amounts of impurity to be trapped relative to the impurities concentration in the bulk solution (i.e. large k_e values). Reid[14] summarizes a number of systems analyzed using this theory. In general, though, the above mechanism can only account for impurities less than about 10^{-4} mole percent.

Wilcox,[15] using a boundary layer model, produced analytical solutions for the concentration profiles of solvent and solute from the bulk solution to the crystal. The model implied that the solid-liquid interface was planar, and that no transverse concentration gradients existed. However, several investigators[16,17,18,19] of solid-solution forming systems of metallurgical interest reported that the interface was not always planar, but rather a cellular structure often existed with transverse concentration gradients. Cheng _et al_.[20] studied several organic systems and verified that the breakdown of the planar interface could be predicted by the so-called constitutional supercooling criterion of Rutter and Chalmers.[16] They also observed occlusion formation and suggested that solution or melt trapping could be accounted for by a rough or dendritic interface.

The constitutional supercooling criterion is illustrated in Figure 4. As crystallization occurs, one

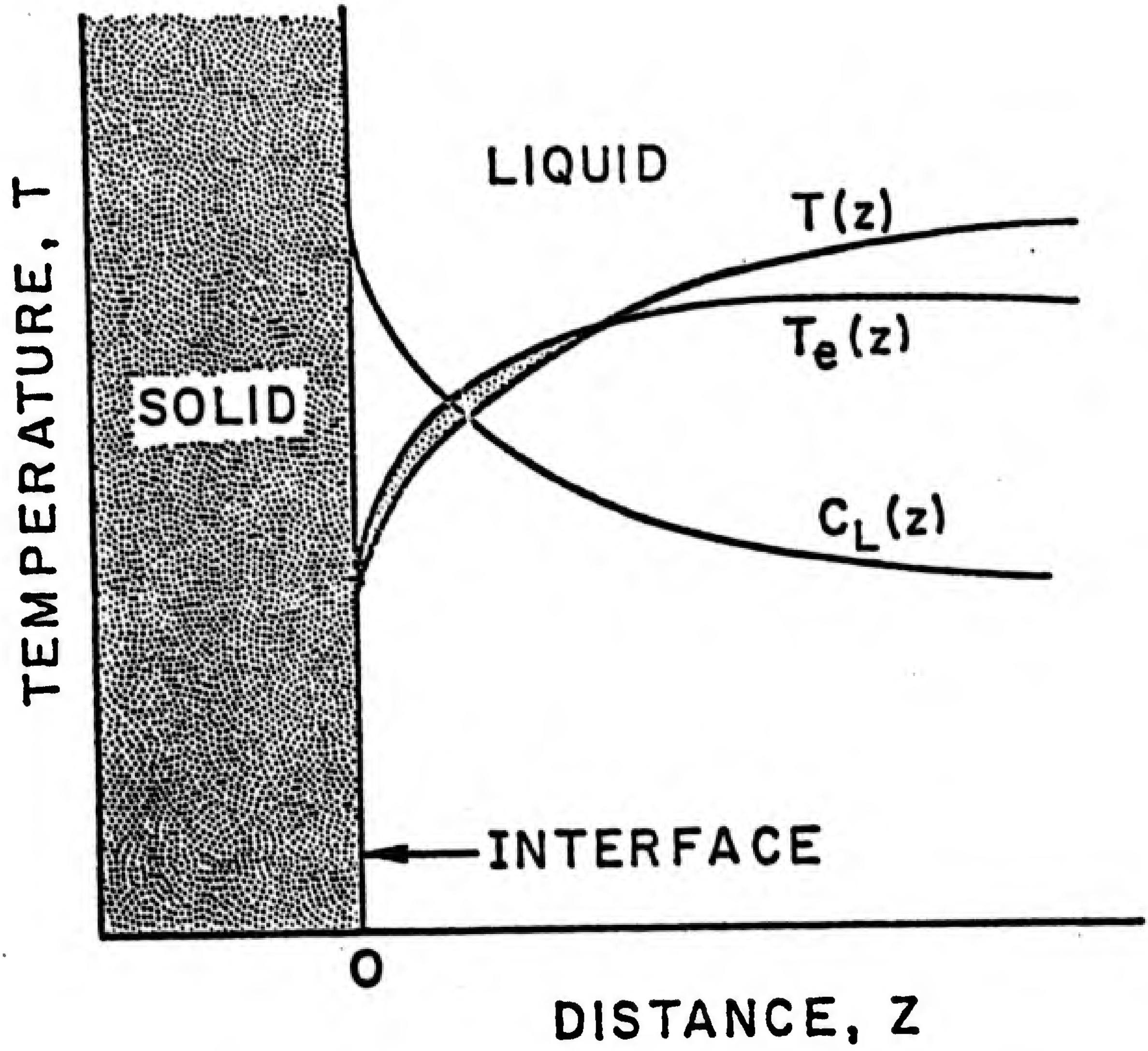

Figure 4. Constitutional supercooling.

component is rejected at the interface. If the diffusion of that component away from the interface is slow compared to the rate at which it is rejected, a concentration gradient will form from the bulk liquid to the interface as shown by the line $C_L(Z)$. It is known from the thermodynamics that the equilibrium freezing temperature decreases as the impurity concentration increases. This decrease in equilibrium freezing temperature is demonstrated by the line $T_e(Z)$. The driving force for crystal growth is the undercooling, $T_e(Z) - T(Z)$, where $T(Z)$ is the actual liquid temperature. Thus a temperature field has been imposed on the system which is represented by the line $T(Z)$, with the undercooling represented by the shaded area. For the conditions shown, the undercooling is seen to be larger some distance away from the interface than at the interface itself. Therefore, when a new crystal layer begins to form, the driving force will be greater in the z direction and the crystal will favor growing out as a spike or dendrite instead of forming a new layer at the interface. Chalmers[21] derived a quantitative criterion to predict the onset of an unstable planar interface. This equation is

$$\frac{G}{V} < m \frac{C_L(\infty)}{D} \frac{1 - k_o}{k_o} \qquad (4)$$

where

$G = \frac{dT}{dZ}$, the imposed temperature gradient at the interface

m = slope of the liquidous line on the phase diagram

Equation (4) shows that for a given G/V ratio, there is a threshold bulk concentration which when exceeded will cause instability.

The constitutional supercooling criterion is based on the thermodynamics of the system. It neglects the effects of heat transfer to the solid, the latent heat of fusion of the freezing solid, surface energy effects on the equilibrium freezing temperature, and the kinetics of the crystallizing system. Attempts to correct these deficiencies were later made. These include the perturbation theory of interfacial stability developed by Mullins and Sekerka.[22,23] By incorporating the appropriate heat and mass transfer equations, they were able to investigate whether a perturbation would grow (resulting in a dendrite) or die out.

B. Quantitative Studies of Impurity Trapping

The preceding has shown that crystalline interfaces could become unstable, resulting in dendritic growth. The same conditions causing dendrites could be prevalent on primary dendrite surfaces and thus, dendrites could side branch and eventually grow together. Pockets formed by impinging side branches could trap enough solvent to account for the non-equilibrium amounts of impurity which have been reported by several investigators. The next efforts made in the study of solvent trapping were to determine the conditions which caused occlusion formation and to quantitatively predict the amount of impurity or solution trapped.

Edie and Kirwan[6] studied trapping during unidirectional solidification from the melt. Their technique permitted an accurate control of the crystal growth velocity and the imposed temperature gradient. They used a micro-interferometer to measure the interfacial liquid composition. The solid composition was found to be far from the predicted equilibrium value. They proposed a theory based on trapping by a dendritic interface to account for their results.

By incorporating information in the literature on dendrite radii and spacing, they proposed a correlation to quantitatively predict impurity trapping as a function of crystal growth rate and temperature gradient. The relation they obtained was

$$\left[\frac{k_a - 1}{k_o - 1}\right]^{1/2} = A_1\left[\frac{Dk_o}{m(1 - k_o)}\right]^{1/2} \left[\frac{1}{C_L(\infty)V}\right]^{1/2} + A_2G^{1/2} \qquad (5)$$

where

k_a = apparent distribution coefficient $(C_L(o)/C_S(o))$

D = impurity diffusivity

m = slope of liquidous line on phase diagram

G = interfacial temperature gradient

V = cyrstal growth velocity

$C_L(\infty)$ = bulk liquid (impurity) composition

A_1, A_2 = constants

They tested this theory with experimental data from organic systems and obtained good agreement with A_2 equalling zero. From this, they concluded that the interfacial temperature gradient had no effect on impurity trapping in organic systems.

Ozüm and Kirwan[10] crystallized ice by progressive freezing of stirred solutions of sodium chloride and of sucrose. The interfacial conditions were calculated using a one-dimensional boundary layer model and later correlated with the theory of Edie and Kirwan.[6] It was found that the interfacial temperature gradient influenced the separation in these systems.

Myerson[2] developed a computer simulation of dendritic crystal growth from solution. Thus he was able to modify the theory of Edie and Kirwan[6] by allowing for side branching of dendrites, the complex interactions of heat and mass transfer in the liquid, and the interfacial crystallization kinetics. He employed the computer program to simulate the dendritic growth both from melts and solutions and was able to determine trapping as a function of growth velocity and other process variables. The dimensionless correlation which he proposed is:

$$\left(\frac{1-k_a}{1-k_o}\right)^{1/2} = K_1\left(\frac{\left(\frac{H_f}{C_p}\right)^{n+1} K_V}{VC_L(\infty)m}\right)^{1/2}\left(\frac{D}{\alpha}\right) + K_2\left[\frac{G\alpha}{[mC_L(\infty)]^{n+1}K_V}\right] \qquad (6)$$

where

C_p = specific heat of liquid

H_f = heat of fusion

K_V = constant in kinetic growth expression

α = thermal diffusivity

n = temperature dependence of kinetic growth expression

K_1, K_2 = constants

This correlation differed from that of Edie and Kirwan[6] primarily in the dependence of trapping on the interfacial temperature gradient.

Myerson[2] found that the experimental results of both Edie and Kirwan[6] and Ozüm and Kirwan[10] for trapping during growth from melts were well correlated by Equation (6). Further, he conducted experiments on the trapping of excess water during the growth of single crystals of NaCl, $CaSO_4 \cdot 2H_2O$, and $KAl(SO_4)_2 \cdot 12H_2O$ in a flow crystallizer. He found trapping in all cases and found that the apparent distribution coefficient was correlated with Equation (6). The computer simulation was also able to provide reasonable estimates of the constants K_1 and K_2, although these constants differed for each crystallizing system.

Because Myerson's correlation can adequately describe solvent trapping, not only in the crystallization of single crystals from solution, but also of crystals grown from the melt, the stage was set for the next questions which were asked. Does the phenomenon of solvent trapping occur in a continuous suspension crystallizing system, which is more typical of those used industrially? If so, can the correlation of Myerson be used to predict the extent of such occurrences? This study was undertaken to explore the above questions and to, perhaps, provide information which would be applicable to industrial operations.

Since Myerson suggested that the most influential system parameter in the occurrence of solvent trapping was the crystal growth velocity, an adequate means of determining this value during crystallization in a suspension was necessary. The next section provides the theory most often used in kinetic studies of continuously crystallizing systems. It will also be shown in a later chapter that conditions could be obtained in the suspension crystallizer wherein the crystallization was kinetically controlled.

C. Theory of the Continuous Mixed-Suspension, Mixed-Product-Removal Crystallizer

What is now needed is a suitable theory for determining the crystal growth velocity in order to investigate trapping as a function of this parameter as suggested by Myerson. Because continuous crystallization yields a distribution of sizes, the theoretical applicability of such a theory must hold over the required range. Randolph and Larson[24] developed such a theory which they presented in 1962.

In this theory, the nucleation and growth kinetics, as well as the operating conditions of the crystallizer, are related to the crystal size distribution (CSD). The characterizing variable for the distribution is called the population density of the crystal distribution, n. The complete derivation of the theory is contained in Randolph and Larson.[25] What will be presented here is its applicability to a continuous mixed-suspension, mixed-product-removal crystallizer (CMSMPR). Such a vessel may be represented schematically as in Figure 5.

Consider now a crystallizer of volume, v, which is continuously fed at a rate Q_i and in which crystals are distributed in the mother liquor as shown in Figure 5. In general, seed crystals may be present in the feed stream and both nucleation and growth are occurring within the volume v because of the existing supersaturation. It should be noted that the supersaturation may be as a result of cooling of the solution, evaporation of solvent, or because of chemical reaction. The remaining discussion will be

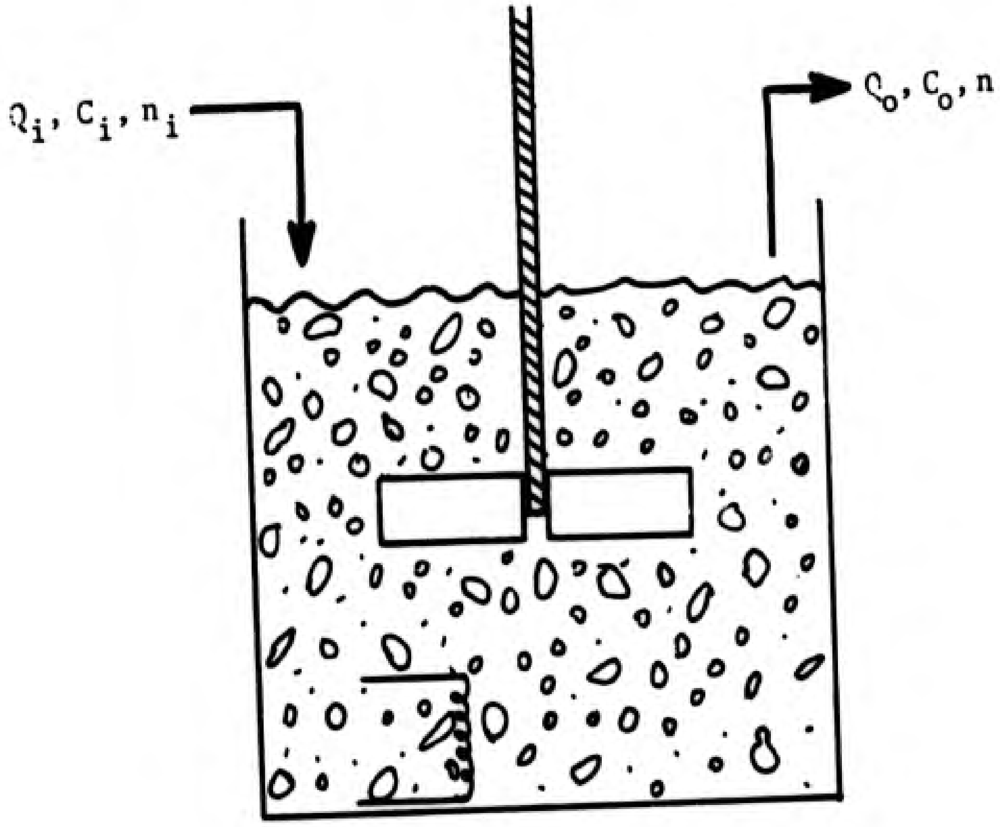

Figure 5. Schematic representation of an MSMPR crystallizer.

restricted to our experimental system, which is of the cooling type, but will in general apply to the other types as well.

The growth rate of crystals, $\frac{dL}{dt} = V$, is usually represented by the change of one characteristic linear dimension, L. This size (L) will be the size of a standard screen through which the crystal just passes. If the crystal shape (habit) is the same for different sizes, as is commonly observed, the volume, mass, or area of a crystal can be determined with the use of an appropriate geometric shape factor. Randolph and Larson[25] define the population density function, n(L), such that the number of crystals in the size range from L to L + dL is given by n(L)dL. Therefore, the number of crystals between two finite sizes L_1 and L_2 is given by

$$\Delta N = \int_{L_1}^{L_2} n(L)\,dL \tag{7}$$

where

ΔN = number of crystals in size range L_1 to L_2 per unit volume of suspension

n = population density (# length^{-1} volume^{-1})

L_1, L_2 = two screen sizes

What remains yet to be determined is the functionality of n with respect to L. The subsequent analysis of this dependence is based upon the following assumptions:

1. The crystallizer is perfectly mixed.
2. There is no classification at the withdrawal, i.e. the probability that a crystal will leave in the exit stream is the same for all sizes.
3. Crystal breakage is assumed negligible.
4. Crystals exhibit a uniform shape factor.

In addition, the usual constraints of steady-state operation require that the feed rate, composition, and temperature remain constant, and that the crystallizer temperature and volume also are held constant.

Most dynamic systems are studied using mass and energy balances. Because of the nature of the system and the need to characterize it using a population density function, it is the number of crystals in a given size range which must be conserved at the steady-state. From the crystal "population balance," the relationship between n and L is determined. It will also be shown that the conservation of mass will be invoked as a constraint on the population density.

The form of the size distribution for an arbitrary size range L_1 to L_2 in the crystallizer volume v, and having population density n_1 and n_2 at sizes L_1 and L_2 respectively is next derived. The growth rate of crystals of size L_1 is V_1 and V_2 for that of size L_2. Keeping in mind that, at the steady-state, the number rate of crystals entering a given size range must equal the number rate leaving that range, then for an increment of time Δt, the number of crystals growing into a size range is

$$vn_1V_1\Delta t \tag{8}$$

and the number leaving

$$vn_2V_2\Delta t \tag{9}$$

If the feed stream contains seed crystals in this range, the input in the volume v is

$$Q_i\bar{n}_i\Delta L\Delta t \tag{10}$$

where

Q_i = volumetric flow rate

$\bar{n}$ = average population density of range L_1 to L_2 in feed

$\Delta L = L_2 - L_1$

Assuming mixed removal, the subscripts may be dropped from the output, and the number removed by bulk flow of crystals in this size range is

$$Q\bar{n}\Delta L\Delta t \tag{11}$$

Combining Equations (8), (9), (10), (11) results in the numbers balance: input to size range ΔL = output from size range ΔL, represented by Equation (12).

$$Q_i\bar{n}_i\Delta L\Delta t + vV_1n_1\Delta t = Q\bar{n}\Delta L\Delta t + vV_2n_2\Delta t \tag{12}$$

Eliminating Δt and rearranging yields

$$v(V_2n_2 - V_1n_1) = (Q_i\bar{n}_i - Q\bar{n})\Delta L \tag{13}$$

Taking the limit as ΔL approaches zero we have

$$v\,\frac{d(Vn)}{dL} = Q_in_i - Qn \tag{14}$$

If the feed is void of seed crystals, or at least has no crystals in the range L_1 to L_2, $n_i = 0$ and Equation (14) reduces to

$$\left(\frac{v}{Q}\right)\frac{d(Vn)}{dL} + n = 0 \tag{15}$$

Next, applying McCabe's ΔL Law[26], which assumes that the linear growth rate, V, is not a function of crystal size (L), and defining the residence time, $\tau = \frac{v}{Q}$, Equation (15) becomes

$$V\tau\left(\frac{dn}{dL}\right) + n = 0 \tag{16}$$

The integral form of this equation is

$$\int_{n^*}^{n} \frac{1}{n}\,dn = -\int_{L^*}^{L} \frac{1}{V\tau}\,dL \qquad (17)$$

where n* is the population density of crystals corresponding to the size of the smallest standard sieve, L*. Randolph and Larson[25] derive Equation (17) using the lower limit of integration to be size $L = 0$, while defining an n^o as the population density of embryo sized nuclei corresponding to $L = 0$. Equation (17) as written will be integrated over the size range of crystals which can be experimentally determined, and hence, extrapolation to $L = 0$ is not necessary.

We see now that the integration of Equation (17) provides the number distribution of the crystal product in a crystallizing system which satisfies the assumptions and constraints which were incorporated into its derivation. Its form is then

$$n = n^* \exp\left(\frac{L^* - L}{V\tau}\right) \qquad (18)$$

Randolph and Larson[25] indicate that laboratory scale crystallizers, and even large industrial scale ones, approximate these conditions well and produce size distributions which can be represented by Equation (18).

By taking the logarithm of Equation (18) it is possible to obtain the linear relation

$$\log n = \left[\log n^* + \frac{L^*}{2.303\ V\tau}\right] - \frac{L}{2.303\ V\tau} \tag{19}$$

Randolph and Larson[25] next proceed to derive the moments of the distribution as characterized by Equation (18). The most significant of which is the third moment

$$\int_{L^*}^{\infty} L^3 n^* \exp\left(\frac{L^* - L}{V\tau}\right) dL \tag{20}$$

Multiplying Equation (20) by a volumetric shape factor, k_V, represents the specific volume of crystals inthe distribution. If this is in turn multiplied by the crystal mass density, the result is an expression for the total mass of crystals per unit volume in the distribution. Denoting this quantity as M_T, the expression becomes

$$M_T = k_V \rho \int_{L^*}^{\infty} L^3 n^* \exp\left(\frac{L^* - L}{V\tau}\right) dL \tag{21}$$

where

M_T = total solids contained in a liter of slurry

k_V = volumetric shape factor

ρ = mass density of crystal

L^* = smallest standard sieve size

n^* = population density at size L^*

Upon integration, Equation (21) becomes

$$M_T = 6\rho k_V n^* (V\tau)^4 \left(\frac{(L^*/V\tau)^3}{6} + \frac{(L^*/V\tau)^2}{2} + \frac{L^*}{V\tau} + 1 \right) \tag{22}$$

Now the kinetics of the crystallizing system can be related to Equations (19) and (22). From a sieve analysis of the crystal product, weight fractions corresponding to

$$W = M/M_T \tag{23}$$

where

M = mass of crystal with average size, $\bar{L}$, of the mean opening of the sieve above and below the sample

M_T = total mass of crystal on a liter slurry basis

W = mass fraction in the size range of the sieve above and below the sample

can be determined within specific size ranges. When the total slurry volume is known, the population density of a size range on a liter of slurry basis may be calculated from

$$n = \frac{W}{\rho k_V \bar{L}^3 \Delta L} \qquad (24)$$

where

$\bar{L}$ = mean size between successive sieves

ΔL = size range between successive sieves

Once the corresponding n's are calculated, a linear plot of Equation (19) as log n vs $\bar{L}$ yields an intercept of $\left(\log n^* + \frac{L^*}{2.303\ V\tau}\right)$, and the crystal growth velocity, V, can then be determined from the slope, which is $-\frac{1}{(2.303)\ V\tau}$.

From a least squares fit of the linear data, n* may be computed for the size of the smallest standard sieve. Using the growth velocity, V, as determined above and n*, a theoretical M_T may be calculated for comparison with the independently measured experimental value. In this manner the conservation of mass is used as a constraint on the population balance.

Murray and Larson[27] have used this technique to report the steady-state kinetics of the ammonium alum-ethanol-water system. Koros, Dalrymple, Kuhlman, and Brockmeir[28] have reported the kinetics of the sodium chloride brine-ethanol system using the preceding technique. Randolph and Rajagopal[29] studied the kinetics of the potassium sulfate-water system employing a Coulter counter for in situ measurement of crystals in the range 0-50 micron. Numerous other studies have demonstrated the usefulness and reliability of the theory as presented by Randolph and Larson.[25]

Now that a reliable analytical tool has been established for measuring the growth velocity of crystals in a continuous system, the remainder of this work will be devoted to the experimental procedures and the analysis of the data thereby obtained.

CHAPTER III

EXPERIMENTAL APPARATUS AND PROCEDURE

The theory for determining the crystal growth velocity in a continuous mixed-suspension, mixed-product removal crystallizer, as outlined in the preceding chapter, employs several assumptions. These constraints must be dealt with in the design of the experimental system. They may be summarized as:

1. The crystallizing suspension must be well-mixed.
2. There is no classification at the withdrawal.
3. There are no seed crystals introduced in the feed.
4. Temperatures are accurately maintained.
5. The crystallizer is operating at steady-state.
6. Crystals exhibit a uniform shape factor.
7. The growth velocity is independent of size.
8. Crystal breakage is negligible.

From these, it would appear that the system design could be made to conform with constraints 1-5, and that an intelligent (a priori) choice of the crystallizing system could account for 6 and 7. The constraint that crystal breakage is negligible remains, and thus will be assumed true, as the task of determining and controlling breakage appears unmanageable.

A. The Experimental CMSMPR System

Aluminum potassium sulfate dodecahydrate ($KAl(SO_4)_2 \cdot 12H_2O$)-water was chosen as our crystallizing system. The choice was made so that trapping results as a function of crystal growth velocity could easily be compared with those of Myerson.[2] Additionally, of the three systems studied by Myerson, potassium alum exhibited the highest growth velocities. The alum used in this study was reagent grade, manufactured by the J. T. Baker Chemical Company.

The crystallizer was designed using a draft tube and three vertical baffles to maintain a well-mixed suspension. The design is similar to those described by Randolph and Larson[25] and has been used reliably by a number of authors.[27,28,31,32] The vessel was made of 1/4 inch plexiglas and had a total volume of 10.8 liters. A cooling coil was wrapped around the draft tube, through which the coolant water was circulated by a Masterline model 2095 bath and circulator, manufactured by Forma Scientific, Inc. Additional baffles were mounted inside, at the top of the draft tube to minimize air entrainment from the vortex created by the impeller. The components and dimensions of the crystallizer, are shown in detail in Figures 6 and 7. The agitation was provided by a Lightnin model L mixer using a three inch diameter, three blade marine impeller.

The mixing of the suspension was noted to be sensitive

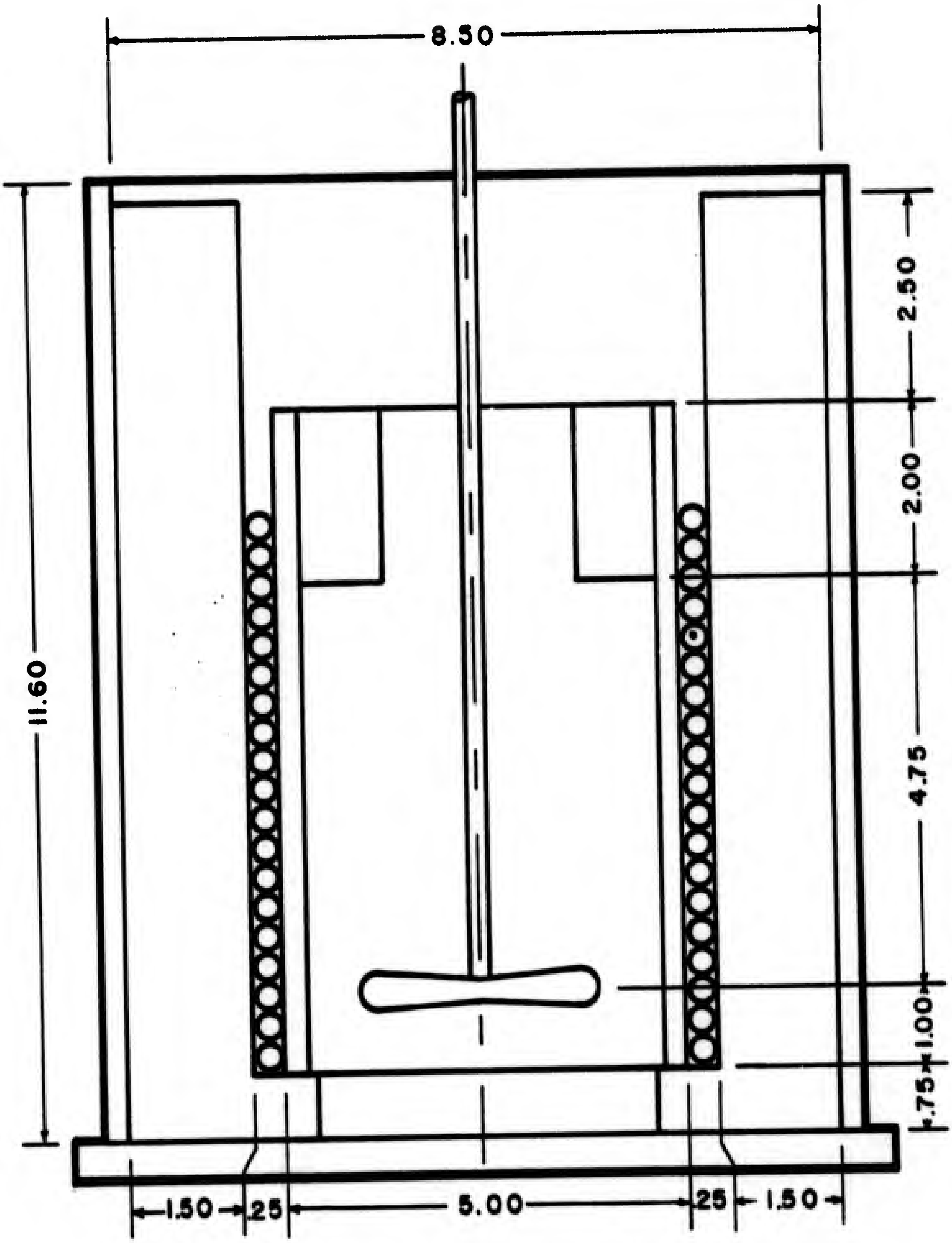

All measurements in inches.

Figure 6. Crystallizer, front view.

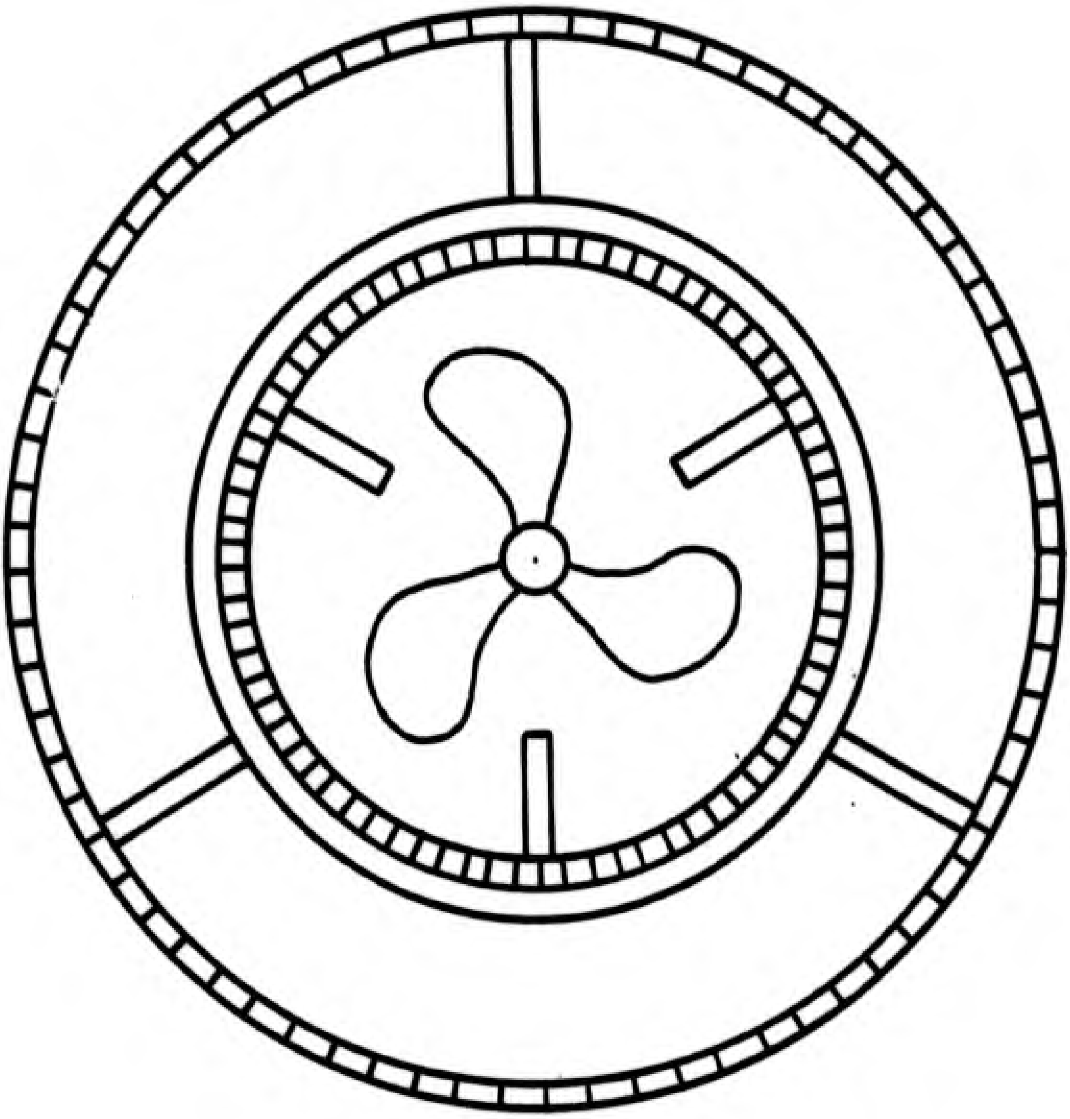

Figure 7. Crystallizer, top view.

to the length and positioning of the draft tube, as well as, to the relative position of the impeller. The location of these components was determined after observing the quality of the mixing in several glass bead-water suspensions.

Initially attempts were made to use an overflow to maintain the operating volume of the crystallizer. It was found, as suggested by Randolph and Larson,[25] that this resulted in product classification at the withdrawal tube. Samples of the overflow differed greatly in density from those of the crystallizer contents which were extracted under vacuum. To eliminate this condition, Randolph and Larson[25] suggest using an electrical contact to activate a withdrawal pump to maintain the liquid level. In this manner, high velocities can be achieved through intermittent withdrawal, and classification can be avoided. The crystallizer was therefore designed with an electrical contact which operated a time delay relay. When the relay was closed, a timer was activated which controlled a Cole-Parmer Masterflex pump which maintained the crystallizer at an effective volume of 8.5 liters. The details of this control system are shown in the schematics of Figures 8 and 9. The withdrawal and sampling tubes were 0.3 inch I.D. and were placed in the annular space, between the vertical baffles, and on opposite sides of the vessel to a height of 4 inches

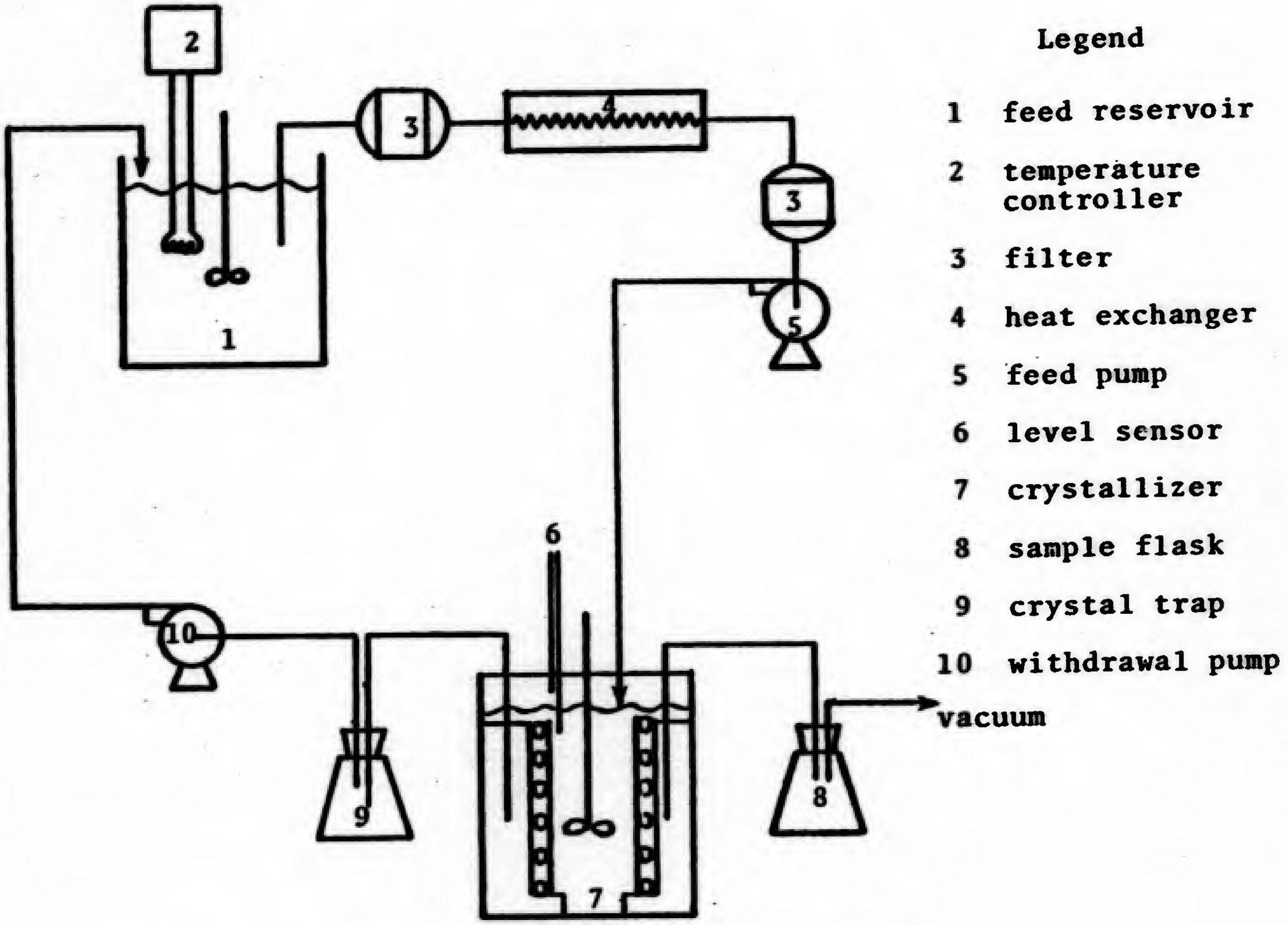

Figure 8. Schematic of crystallization apparatus.

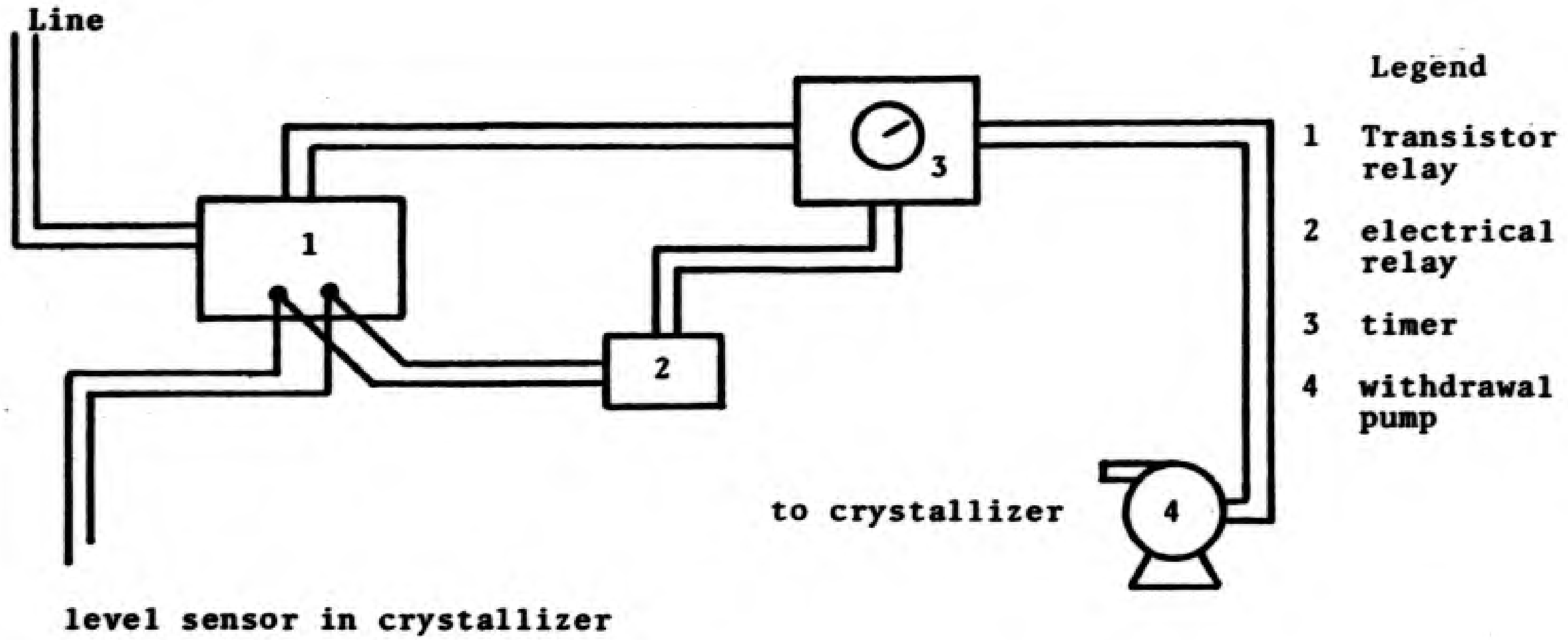

Figure 9. Schematic of level control system.

above the bottom. These tubes were omitted from Figure 6 for the sake of clarity.

From preliminary experiments it was noted that 20 mesh crystals were about the largest grown. The settling velocity for 800 micron alum crystals in saturated alum solution was calculated from Equations 7-51 and 7-54 of McCabe and Smith[30] to be 6.8 cm./sec. The corresponding flow rate for the 0.3 inch I.D. pipe and tubing is 173 cc./min. The withdrawal pump was then set to remove 500-550 cc./min. (roughly 3 times the settling velocity) to insure rapid withdrawal without classification. With this arrangement, the crystallizer volume fluctuated ±5% over time. To eliminate the problem of ruptured tubing in the peristaltic pump, a crystal trap was included in the design. The trapped slurry was stirred and heated to dissolve the crystals, and clear liquor was siphoned and returned to the feed tank.

The feed tank was a 17 liter plastic vessel which used a Haake Model E51 immersion temperature controller and circulator to maintain the saturation temperature and concentration. A Fisher laboratory stirrer was used to mix and suspend the solids in the saturated solution. The feed was pumped, using a second Cole Parmer Masterflex pump, first through a filter, a heat exchanger, and then through another filter before entering the crystallizer.

The filters were 5 micron (nominal) Ultipor type, manufactured by the Pall Corporation. Through this arrangement, the introduction of seed crystals in the size range of the study was eliminated.

B. Experimental Procedure

The solubility data for potassium alum of Mullin, Garside, and Unahabhokha[33] was used in this study and appears in Figure 17 of Appendix A. Our own measurements and the data in the International Critical Tables were found to be in close agreement with theirs over the temperature range of interest.

At the beginning of an experimental run, the crystallizer was charged with a saturated solution from the feed tank. The system was maintained at this temperature for about one hour before cooling took place. Once the desired operating temperature had been reached and crystallization was observed,the system was operated 6-8 residence times before sampling. During this time, samples of the feed and withdrawal were tested for total solids content. This data was used as a check on the operation of the system. These samples were baked at 220°C and the total solids were determined from the residue. Since potassium alum contains 12 waters of hydration, accounting for 45.5% by weight, which evaporate on baking, the weight of hydrated alum in solution was determined from the following

$$W_c = (1.834)W_b$$

where

W_c = weight of hydrated alum corresponding to residue weight

W_b = weight of baked, dehydrated alum residue

1.834 = 1/0.545 = inverse of weight fraction of alum solids in a sample of hydrated alum

Approximately 500 ml. of slurry were aspirated from the crystallizer for each sample. The slurry was then filtered through a Kimax 600 ml.-90C fritted glass funnel. The funnel pore size is 40-60 microns. Once the mother liquor was filtered out, the remaining crystals were washed with about 100 ml. of acetone to prevent agglomeration or further crystallization. The crystals were then allowed to dry in air for a minimum of 1 hour before sieving. The crystallizer operation was assumed at steady state when the suspension densities of successive samples were in close agreement. In later experiments, the filtrate and additional samples of the crystallizer, withdrawal, and feed, which were removed just after the crystal sample, were tested for total solids content. The baking and testing procedure is as outlined above.

Once dried, the crystals were sized using screens of the U.S. Standard Sieve Series conforming to A.S.T.M. E-11 specifications. The sieves were 3 inch standard pigment screens of 8, 10, 16, 20, 30, 40, 60, 80, 100, 120 and 200 mesh which were manufactured by the Dual Manufacturing Company. The samples were subjected to 10 minutes of screening which was performed partly by hand and partly with the aid of a locally manufactured shaking device.

After screening, the crystals on each sieve were weighed separately and the weight fractions of crystal corresponding to the appropriate size ranges were determined. The population density, n, was calculated using Equation (24). The corresponding least-squares determinations of n vs $\bar{L}$ yielded the linear growth velocity from the slope of Equation (19).

The procedure for testing for occluded water in the crystals was that proposed by Myerson.[2] The air-dried crystals were weighed and then baked at 220°C for several hours. The weight loss after baking was attributed to the evaporation of the water of hydration and the occluded water. The amount of trapped water was determined from the following relation from Myerson[2]

$$I_W = W_c - (W_b + W_b X_{H_2O}) \qquad (26)$$

where

I_W = mass of trapped water

W_c = original hydrated crystal

W_b = mass of baked crystal residue

X_{H_2O} = mass ratio of water to anhydrous alum (gm. H_2O/gm. $KAl(SO_4)_2$) = .834

CHAPTER IV

RESULTS AND DISCUSSION OF RESULTS

Three preliminary experimental runs were conducted to test the apparatus design and to improve on the operating and sampling procedures. The results of these runs were also useful in determining the process conditions for subsequent runs. Our objectives at this point were to demonstrate the performance of the crystallizer as an MSMPR and to achieve high growth velocities and large crystals to test occlusion formation. The product crystals were then to be subjected to intense heating to determine whether trapped solvent was present, and whether such occluded solvent could be correlated with the results of Myerson.[2] In particular, of course, the average linear growth rates for the suspension must be determined for use in the correlation.

A. Determination of Linear Growth Velocities

As indicated earlier, one of the necessary criterion for the calculation of the growth velocity is that the crystal shape be uniform for all sizes. The crystals produced in these experiments were observed to be regular octahedra in all size ranges. As a result, a constant value for the volumetric shape factor k_V, was incorporated into the appropriate calculations for determining the growth velocity. The value of $k_V = 0.471$, as reported by Garside and Jancic[35] for an octahedral geometry, was used.

There were a total of nine regular experimental runs made in conjunction with this study. The applied temperature differences between the saturated feed and the crystallizer ranged from 3 to 15°C, while the residence times ranged from 0.49 to 2.94 hours. The crystallizer temperature varied from 27 to 30.1°C. The corresponding calculated growth rates ranged from 1.26×10^{-6} to 8.02×10^{-6} cm./sec. These results and the corresponding experimental conditions are tabulated in Appendix B.

Figures 10, 11, 12, 13, and 14 exhibit the log n vs $\bar{L}$ plots for a typical sample from each run. (The plots for the remaining samples are contained in the author's laboratory notebook.) From these the growth velocity can be calculated using the Randolph and Larson[25] procedure discussed in Chapter II. The lines are those calculated from the linear least-squares determinations of the data. A summary of the calculated data from an analysis of the above runs is shown in Table 1 of this section. The data of runs 1, 3, 4 and 5 are not included here. Equipment failure was experienced during run 1 while in-line crystallization and pump failure resulted in the

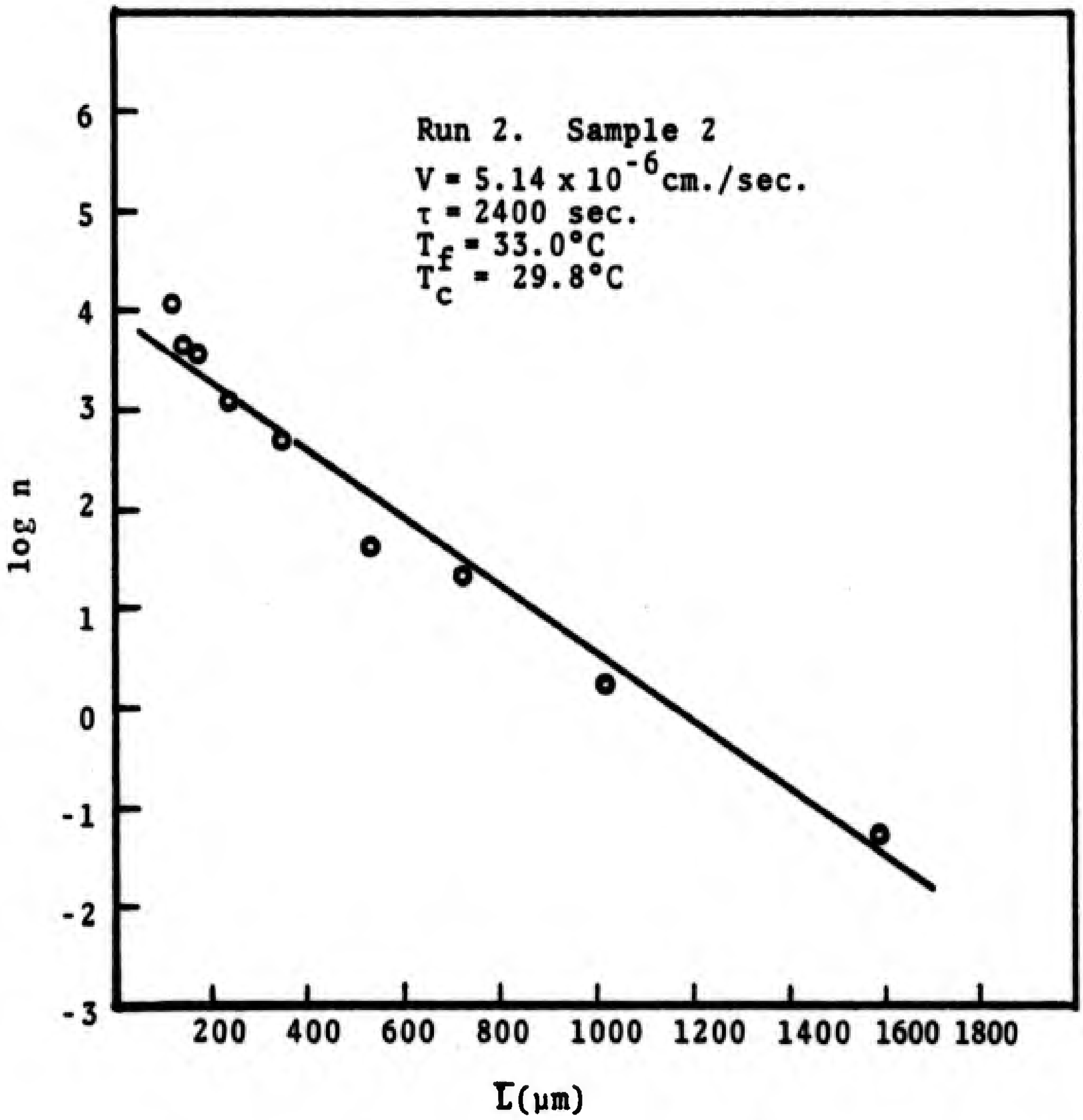

Figure 10. Crystal size distribution.

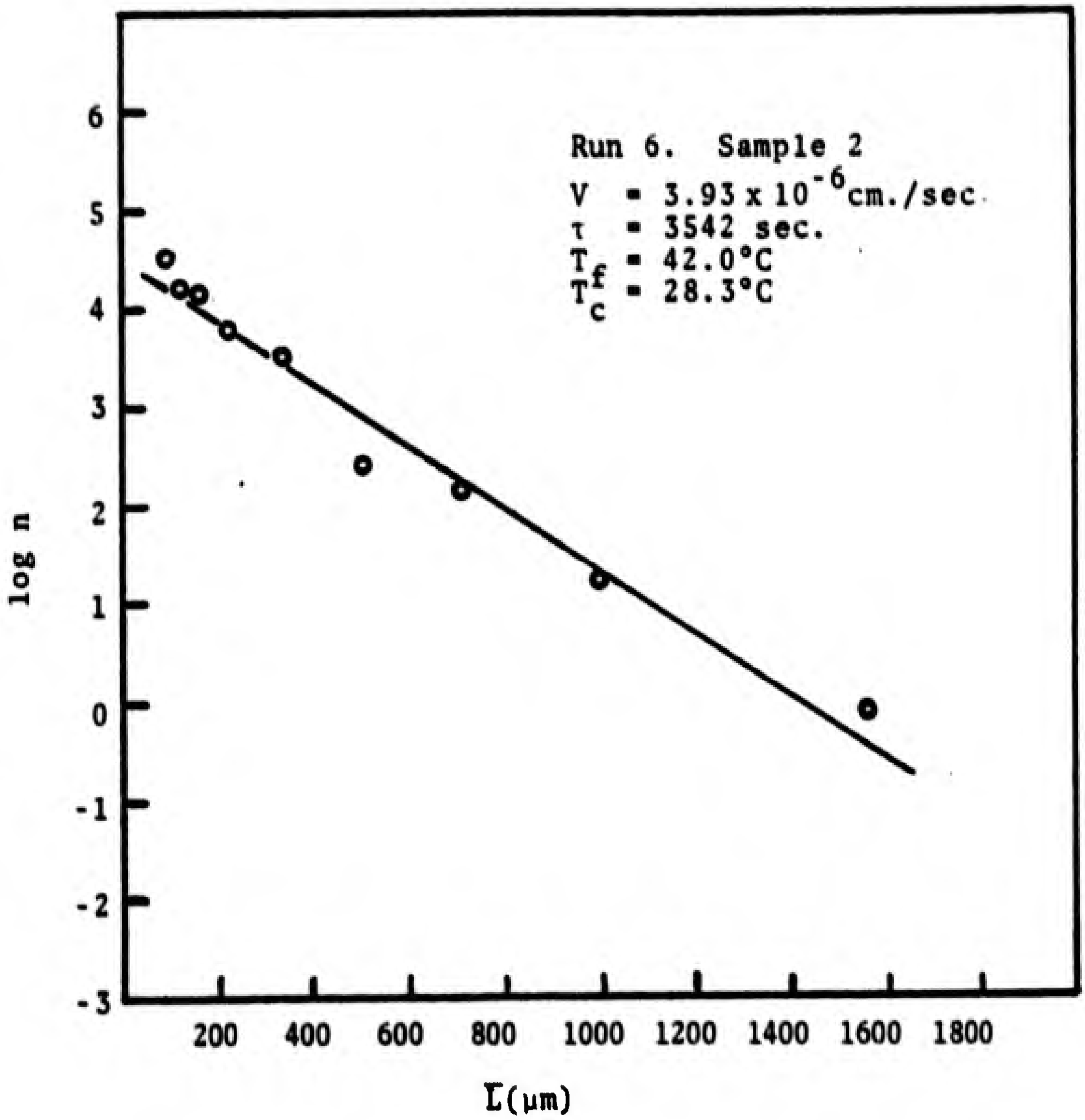

Figure 11. Crystal size distribution.

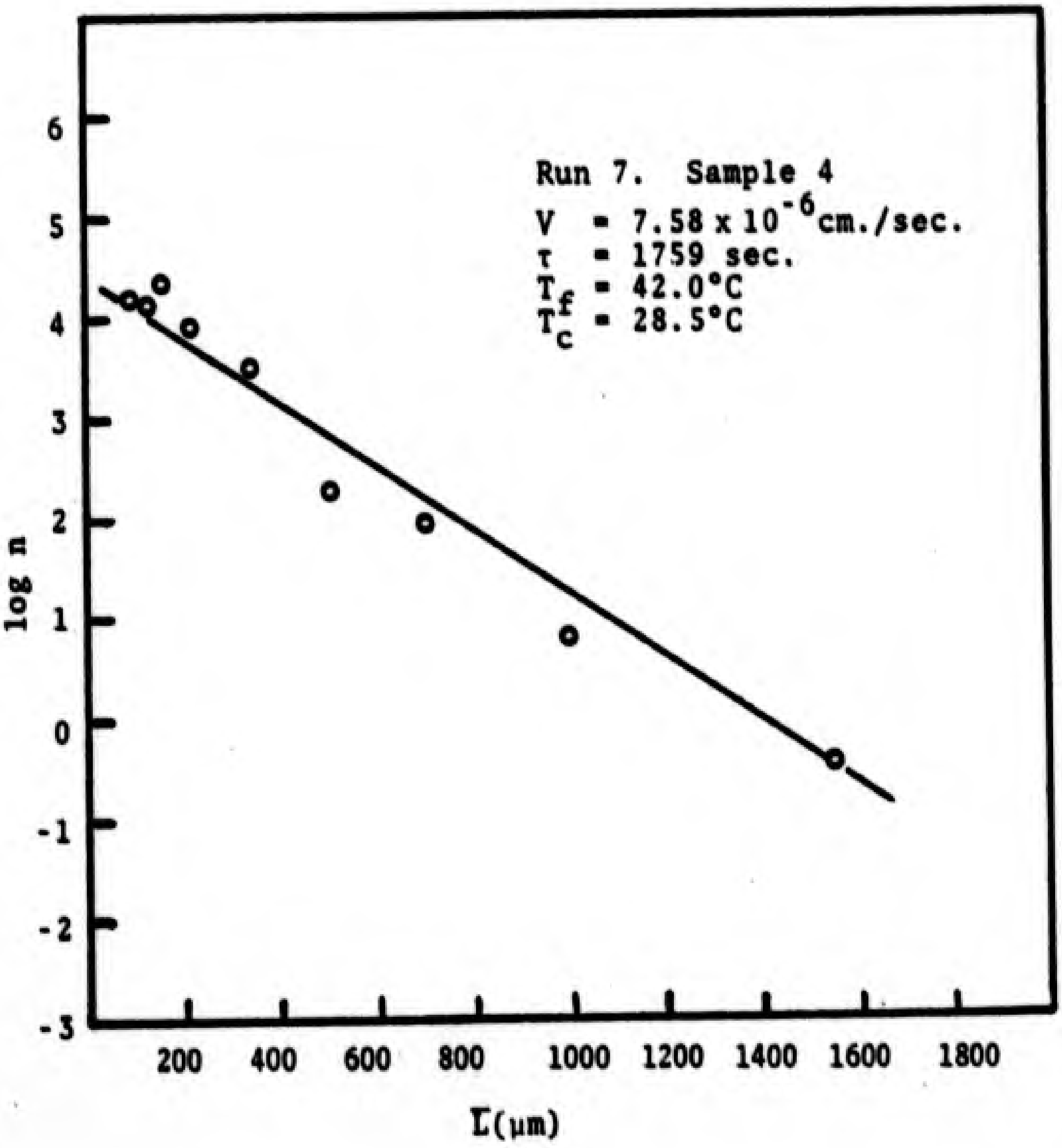

Figure 12. Crystal size distribution.

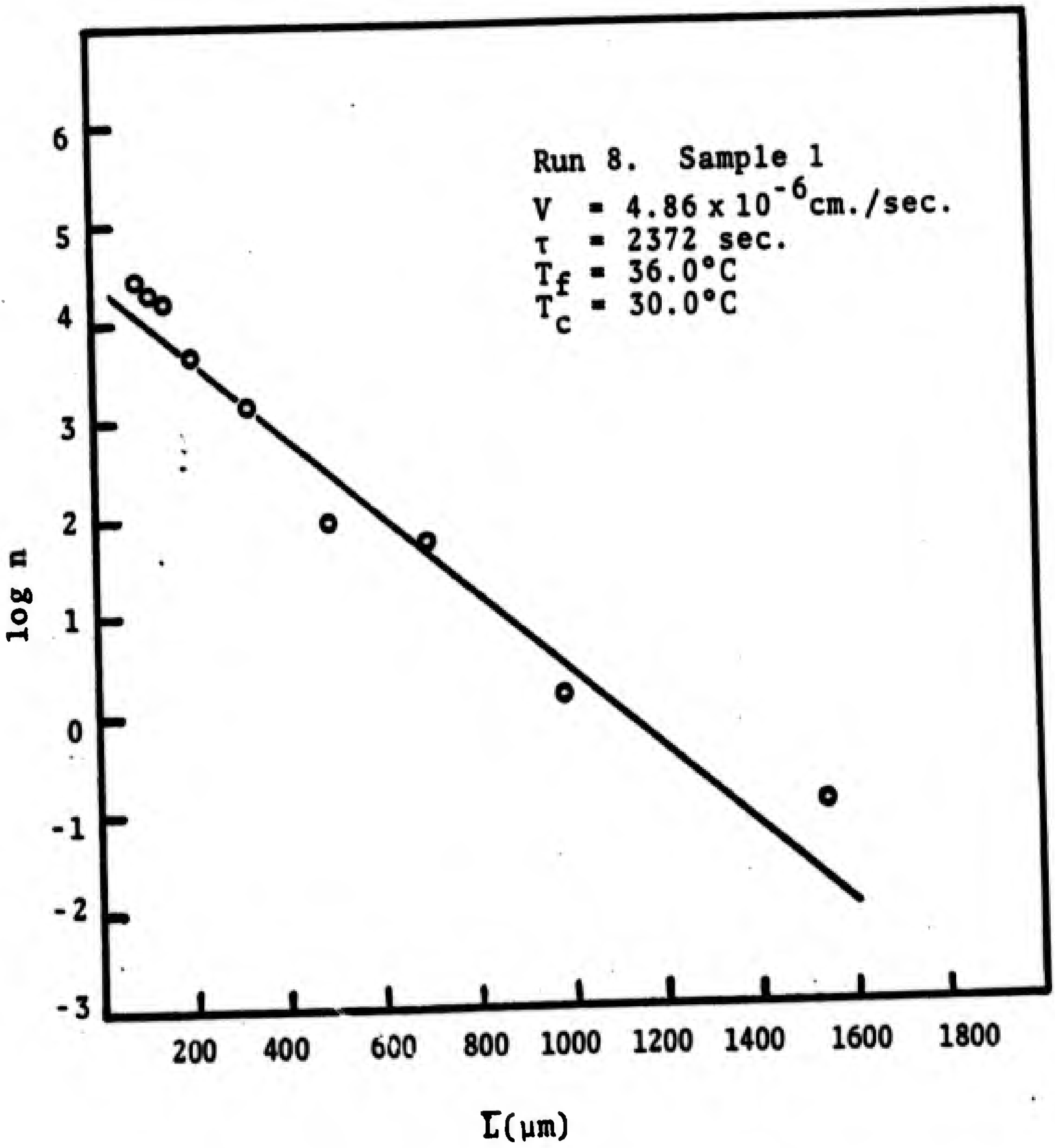

Figure 13. Crystal size distribution.

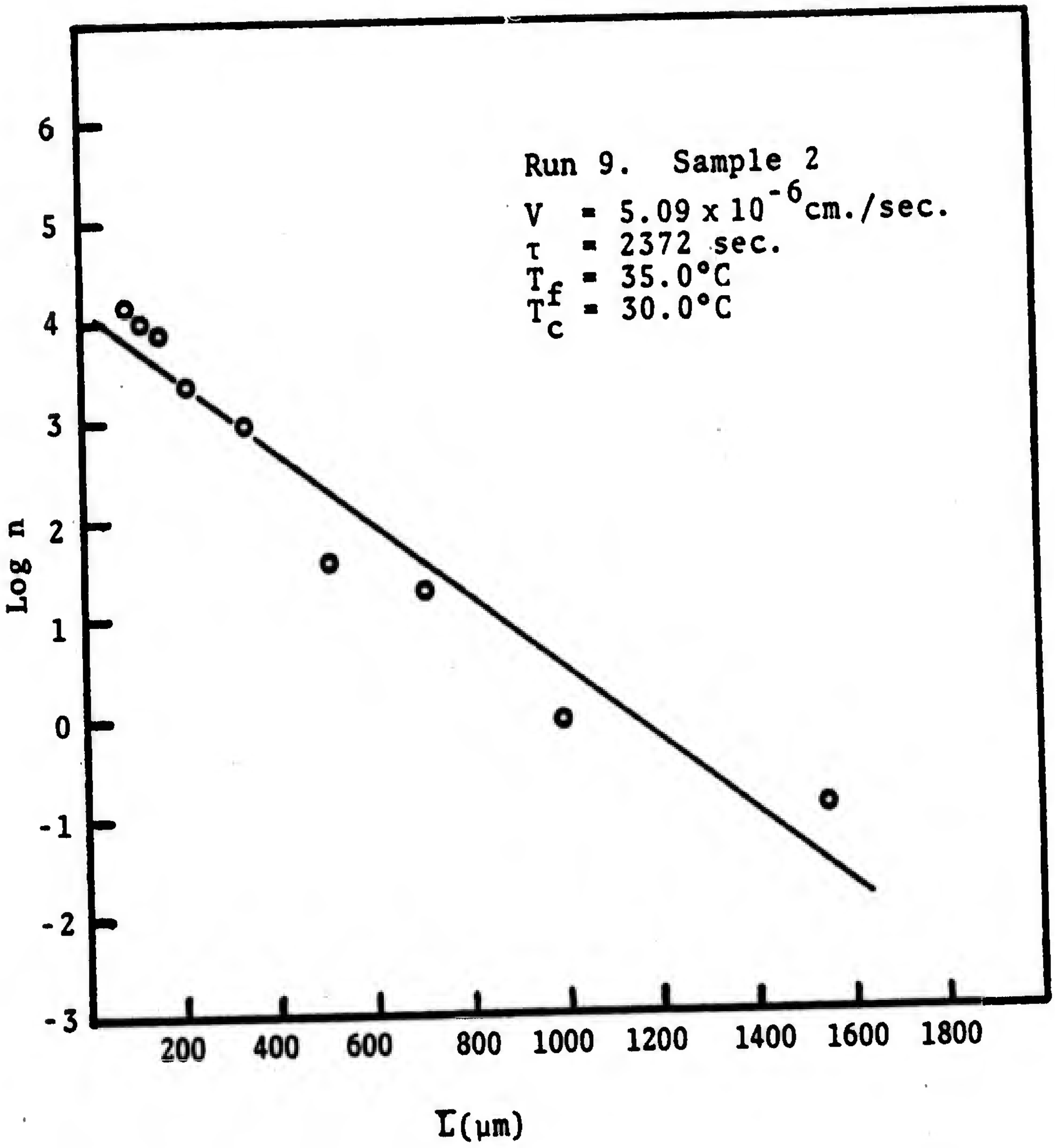

Figure 14. Crystal size distribution.

unreliability of the data of runs 3 and 4. Because of the variation of the suspended solids concentration, M_T, run 5 is believed to have shown oscillatory behavior, and will be discussed separately.

The values of n* in Table 1 were calculated from the least-squares fit of Equation (19). The fitted slope and intercept were incorporated into the linear equation for a value of L = 75 microns (the smallest size measured in this work). Thus n* is the value of the population density for the crystal size corresponding to the smallest observed crystal size.

As was mentioned earlier, Equation (22) should be used as a constraint on the calculation of the growth velocity from the population balance data. The usual technique is to determine what value of n^o (which corresponds to n* when L* = 0 in Equation (22)) is necessary to satisfy the material balance. This value of n^o is further used in a determination of the nucleation rate. Since this study is primarily concerned with the growth velocity and not the nucleation rate, an alternate technique was used to fit the material balance.

The values of n* from Table 1 were used in Equation (22) to determine what values of the growth velocity, V, were necessary to satisfy the material balance exactly. In this manner, the necessary adjustment of V could be

Table 1

Summary of Least-Squares Determinations

Run #	Sample #	τ (sec.)	Growth Velocity x 10^6 (cm./sec.)	n^* (#/μm-ℓ)	Index of Determination
2	1	2400	4.84 ± 0.69**	7,796	0.98
2	2	2400	5.14 ± 0.79	5,079	0.97
6	1	3542	4.01 ± 0.87	21,694	0.98
6	2	3542	3.93 ± 0.62	23,102	0.97
6	3	3542	3.99 ± 0.95	19,566	0.98
7	1	1759	7.25 ± 0.80	32,248	0.95
7	2	1759	8.07 ± 1.13	28,791	0.96
7	3	1759	7.94 ± 1.17	34,076	0.96
7	4	1759	7.58 ± 1.59	20,995	0.98
8	1	2372	4.86 ± 0.67	18,381	0.96
8	2	2372	4.74 ± 0.66	16,253	0.96
9	1	2372	4.52 ± 0.94	11,748	0.98
9	2	2372	5.09 ± 0.54	8,262	0.94
9	3	2372	4.80 ± 0.63	10,125	0.96

**standard deviation of value

compared with the least-squares standard error estimate. As shown in Table 2, the necessary adjustment to the linear growth velocity to satisfy the material balance was within the standard error estimate in all cases but one. The one sample outside this range deviated by less than 1%.

It appears then that the linear growth rates calculated with the theory of Randolph and Larson[25] are compatible with the overall material balance as well. Thus, they should provide reasonable estimates of the actual average growth rates in the suspension within the limits of the validity of the assumptions in the Randolph and Larson analysis. As mentioned in Chapter III and discussed below most of these assumptions could be satisfied by apparatus design and choice of crystallizing system.

The experimental crystallizer and associated equipment are believed to have satisfied the necessary constraints. The series of filters of 5 micron nominal size were certainly adequate to eliminate the introduction of seed crystals in the size range of this study. As noted, the smallest crystals analyzed were 75 microns in diameter. The draft tube, impeller, and crystallizer geometry were sufficient to provide an observable well-mixed suspension. Classification at the withdrawal was a problem in the preliminary runs, but was eliminated by the use of the

Table 2

Results of Adjusting V to Satisfy Material Balance

Run #	Sample #	Required $V \times 10^6$ (cm./sec.)	% difference from experimental
2	1	4.11	17.76
2	2	4.65	10.53
6	1	3.70	8.37
6	2	3.66	7.37
6	3	3.68	8.42
7	1	6.53	11.02
7	2	7.00	15.28
7	3	6.85	15.91
7	4	7.23	4.84
8	1	4.44	9.68
8	2	4.29	10.48
9	1	4.20	7.61
9	2	4.61	10.41
9	3	4.32	11.11

liquid-level control system using an intermittent withdrawal at high flow velocities.

As shown earlier, the withdrawal system was designed to operate roughly at a factor of 3 times the settling velocity of the 800 micron crystals. This was certainly fast enough to overcome the settling velocity of smaller crystals and can be shown to also have been sufficient to remove the largest crystals grown, this size not exceeding 2,000 microns. An experimental measurement was also performed to analyze the total solids being fed into, being withdrawn from, and being sampled from the crystallizer. While the distribution of the withdrawal was not measured (since it ultimately had to pass through a peristaltic pump), it can be argued that close agreement of the total solids in the above samples is sufficient to discount classified withdrawal. The results of these measurements are shown in Table 3. The feed, withdrawal, and additional crystallizer samples were taken immediately after a product sample was removed. The measurements correspond to the appropriate sample number, except in the case of run 2. The above procedure had not yet been initiated and the measurements shown correspond to the conditions at the first sampling. While there is some deviation, the measurements are believed well within the accuracy of the sampling technique and indicate steady state operation, no

Table 3

Measurement of Total Solids Content

Run #	Sample #	Feed (g/1)	Crystallizer (g/1)	Withdrawal (g/1)	Product Slurry + Filtrate (g/1)
2	1	162.24	148.7	-	-
6	1	225.50	211.25	237.67	226.93
6	2	221.43	220.00	221.18	212.20
6	3	220.51	208.69	223.68	213.19
7	1	215.77	204.12	236.17	209.19
7	2	218.39	188.99	219.06	208.90
7	3	243.36	234.46	206.36	216.99
7	4	205.44	196.36	212.80	201.02
8	1	190.66	186.11	182.28	183.43
8	2	187.30	178.96	185.17	218.42
9	1	183.37	178.27	167.22	171.03
9	2	172.12	175.93	170.06	172.73
9	3	176.91	175.23	175.01	173.02

classification of the withdrawal and the crystallizer sample is representative of the tank contents.

The temperature controllers were found adequate to control the feed and crystallizer within ±0.1°C. This was not enough of a variation to affect the steady-state operation of the system. A check on the steady-state is the total solids content of successive samples. This can be verified by the data in Appendix B and will be addressed in more detail later. However, in general 6-8 residence times elapsed between samples to allow the system to return to the steady-state.

These observations and experimental procedures were seen to verify that our crystallizing system could conform to the assumptions of the theory required to calculate the growth velocity. The additional constraints were involved with the choice of crystallizing system rather than design. As previously stated, the potassium alum crystals were uniformly octahedral in all size ranges and the use of a constant volumetric shape factor is justifiable. Additionally, one could postulate more complex growth models (size-dependent growth, etc.) of the suspension crystallizer to obtain different results for growth rates. However, such models would contain additional parameters and there does not appear to be any justification for their use for the purposes at hand. For example, Garside and

Jancic[35] found the potassium alum-water system to exhibit size dependence up to about 500 microns. For larger crystals, the overall growth rate was almost independent of size.

As a further check on our linear growth rates as calculated by the size distribution analysis, the interfacial crystallization kinetics can be extracted from the observed growth rates and the interfacial supersaturation. In order to determine the supersaturation existing at the interface for a given applied supersaturation and growth rate, the mass transfer influence in the crystallizer must be assessed. Under steady-state conditions, the mass transport of solute to the surface of the crystal must equal the rate of incorporation of solute in the crystal. Mathematically this is shown as

$$k_a L^2 k_m (C_b - C_L(o)) = \rho_c k_V \frac{dL^3}{dt} \qquad (27)$$

where

k_a = crystal surface shape factor = .46

k_m = mass transfer coefficient

$(C_b - C_L(o))$ = concentration difference between bulk and interfacial solutions.

ρ_c = crystal density

Since $V = \frac{dL}{dt}$, this may be further reduced to Equation (28)

$$V = \left(\frac{k_a}{k_V}\right) k_m(C_b - C_L(o))/3\rho_c \tag{28}$$

The supersaturation at the interface, $(C_L(o) - C^*_L(o))$ may then be written as

$$(C_L(o) - C^*_L(o)) = C_b - C^*_L(o) - 3\rho_c k_V V/k_a k_m \tag{29}$$

where $C^*_L(o)$ is the concentration of solute that would be in equilibrium with crystal at the temperature of crystallization. Equation (29) now allows the calculation of the interfacial supersaturation provided that the applied supersaturation and growth rate are measured and that values of k_a, k_V, ρ_c and k_m are available. Values of both the area and volume shape factors are provided by Garside and Jancic[35] for potassium alum.

The mass transfer coefficient from solution to a particle in an agitated suspension is well correlated[30] by the equation

$$k_m = \frac{D_V}{L}\left(2 + 0.31\left(\frac{\mu}{\rho_c D_V}\right)^{1/3}\left(\frac{L^3\rho_c\Delta\rho g}{\mu^2}\right)^{1/3}\right) \tag{30}$$

where

D_V = diffusivity of alum in water (cm.^{2}/sec.)

μ = solution viscosity (centipoise)

$\Delta\rho$ = difference between crystal and solution densities

g = gravitational constant (cm./sec.^{2})

The diffusivity and solution densities are reported by Mullin, et al.[33] and the solution viscosity for a 10% volume fraction of solids was estimated using Equation (3-126) of Perry's Handbook.[36] The resulting expression for the mass transfer coefficient for a given size is

$$k_m = (1.006 \times 10^{-5}/L + 3.27 \times 10^{-3})\,\text{cm./sec.} \qquad (31)$$

The mass transfer coefficient as a function of crystal size in the range of interest is shown in Table 4.

In order to obtain the equilibrium solubility, $C_L^*(o)$, the interfacial temperature must be known. Following an analysis similar to that leading to Equation (28), it can be readily shown that the interfacial temperature differs by less than 0.01°C from the bulk temperature.

The applied supersaturation, $(C_b - C_L^*(o))$, was calculated from the actual measurements of the solids content of the feed as shown in Table 3. The equilibrium value, $C_L^*(o)$, was obtained from the solubility diagram at the crystallizer temperature. Consequently, the interfacial growth kinetics (growth rate vs interfacial supersaturation)

Table 4

Mass Transfer Coefficients

Screen Mesh	$\bar{L}$, cm	k_m, cm./sec.	$\overline{k_m}$
			3.645×10^{-3}
-8 + 10	0.218	3.31×10^{-3}	
-10 + 16	0.159	3.33×10^{-3}	
-16 + 20	0.1015	3.36×10^{-3}	
-20 + 30	0.0725	3.40 x 10-3	
-30 + 40	0.05125	3.46×10^{-3}	
-40 + 60	0.03375	3.56×10^{-3}	
-60 + 80	0.0215	3.73×10^{-3}	
-80 + 100	0.0165	3.87×10^{-3}	
-100 + 140	0.0128	4.05×10^{-3}	
-140 + 200	0.00905	4.38×10^{-3}	

can be readily obtained and compared to previous observations of potassium alum growth rates.

The calculated interfacial supersaturations, using an average k_m, and the applied supersaturations $(C_b - C_L^*(o))$ are shown in Table 5 for each of the experimental runs. It can readily be seen that in most cases the growth rates were "kinetically controlled," i.e. the applied supercoolings were only slightly larger than those existing at the interface. In Figure 15 are shown the average values obtained for each run in this study and literature data for potassium alum obtained by Myerson,[2] Botsaris and Denk,[37] and Mullin and Garside.[38] These other studies were measurements of individual crystals or crystal faces in a flow crystallizer. Botsaris' and Denk's[37] data for the slowest growing faces (111) are also shown for comparison.

As can be seen, our kinetic data for the continuous crystallization of potassium alum is in rather poor agreement with that in the literature although the growth velocities are of the proper magnitude. Few, if any, previous works report a comparison of the crystallization kinetics between a continuous suspension and a single crystal system, regardless of the chemical species. Consequently, no trends can be anticipated. Furthermore, our growth velocities are the average for a distribution of crystal sizes based on one model and one theory. The

Table 5

Kinetic Growth Velocities and Supersaturations

Run #	Sample #	$V \times 10^6$ (experimental) (cm./sec.)	$C_b - C_L^*(o)$ (g/1 soln)	$C_L(o) - C_L^*(o)$ (g/1 soln)
2	1	4.84	3.17	2.22
2	2	5.14	3.30	2.29
6	1	4.01	34.36	33.57
6	2	3.93	25.11	24.33
6	3	3.99	24.42	23.64
7	1	7.25	28.88	27.46
7	2	8.07	25.26	23.68
7	3	7.94	40.82	39.27
7	4	7.58	15.71	14.22
8	1	4.86	18.97	18.02
8	2	4.74	20.04	19.11
9	1	4.52	21.44	20.55
9	2	5.09	10.61	9.61
9	3	4.80	15.32	14.38

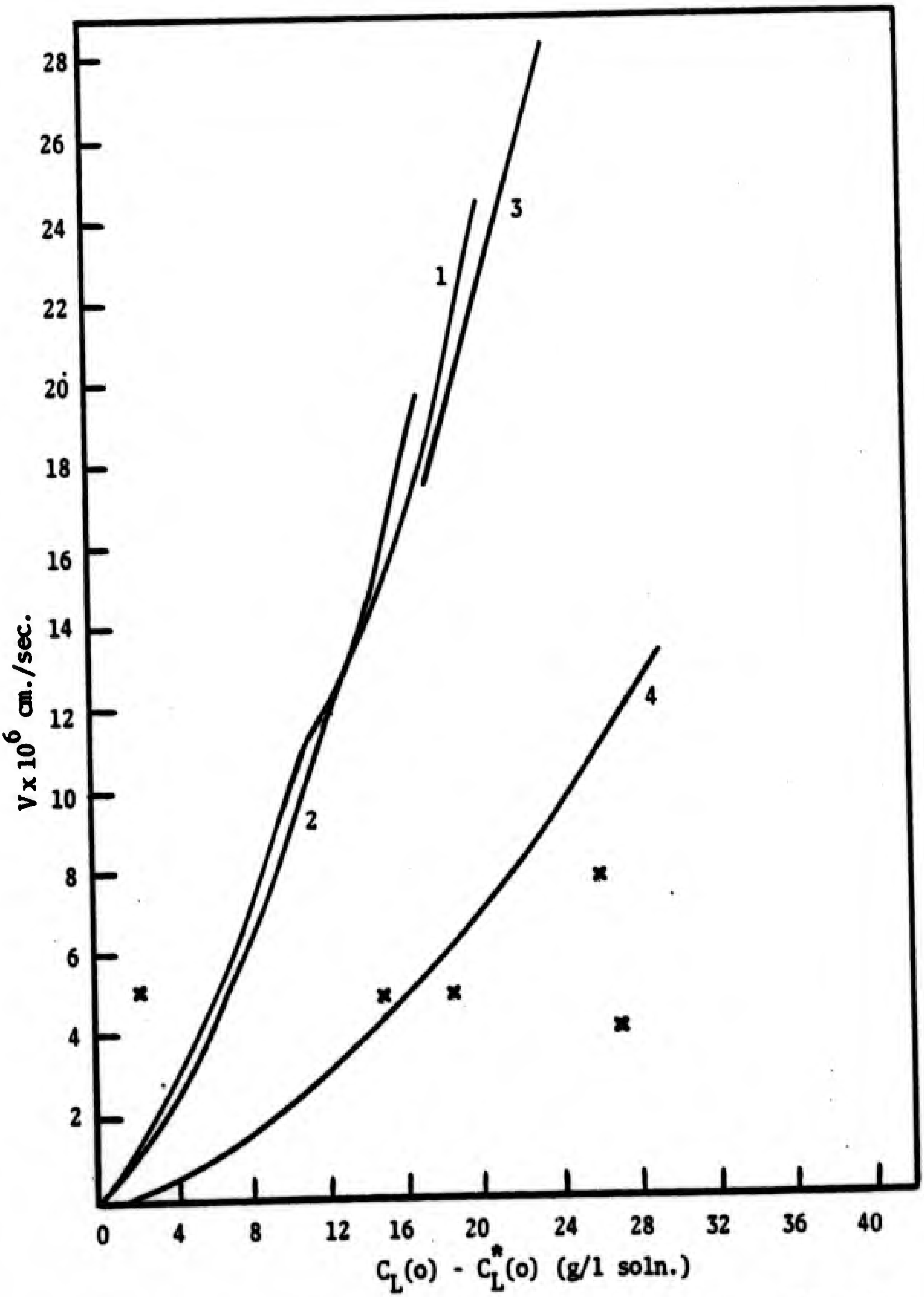

Figure 15. Growth rate as a function of supersaturation - x this study, 1 Myerson,[2] 2 Mullin,[38] Botsaris and Denk,[37] 3 average crystal growth, 4 (111) faces only.

kinetics we have observed may reflect the variability of growth rate at a given supersaturation as was observed by Botsaris and Denk.[37] Alternatively, they may be low owing to an inadequacy of the model chosen.

We have seen that the population balance theory is widely used in kinetic studies. As was mentioned earlier, run 5 is believed to have oscillated. The total solids concentration of the 4 successive samples increased and decreased erratically. (See Appendix B). This is suggested to be an indication of unsteady state operation by Randolph and Larson.[25] Even though this data was suspect, the calculated growth rates were found to be in better agreement between samples of this run than were many of those from other runs. Additionally, the least-squares fits were good and the adjustment of the growth velocity to satisfy the material balance was less than 4% for three of the four samples. For other runs, the adjustment varied from 4.8 to 17.7%.

The oscillations are believed to have been caused by classified withdrawal. Withdrawal pump failure necessitated a replacement midway through the run. A higher velocity centrifugal pump was used, and the solution which was removed to maintain the crystallizer volume was seen to be high in solids content. Since this solution was returned directly to the feed tank, an oscillation could have been initiated which did not dampen out over the remainder of the experiment. The addition of the crystal trap precluded pump failure in subsequent runs.

The point to be emphasized here, is that the log n vs. L plots from least-squares determinations of good fit are not sufficient to indicate steady-state operation. Agreement of the material balances and, hence, total solids concentrations between samples was found to be a better indication of steady-state operation.

After having noted that the theory is seemingly insensitive to suspected poor data, one last constraint should be addressed. Up to this point, crystal breakage has been overlooked.

Under the influence of the agitation necessary to create a "well-mixed" suspension, breakage could have been contributing greatly to secondary nucleation. This would tend to limit the growth rate since growth and nucleation are competing mechanisms. Some of our more qualitative observations also indicate that breakage may have been a prevalent factor. Large increases in the applied supersaturation had little or no effect on the production of larger crystals or on increasing the growth velocities. It could be hypothesized that perhaps when crystals grew beyond a limiting size, they were broken into nuclei sized crystals. The uniformity of all sizes and the smoothness of the crystal faces leads us to believe that crystals were not broken into smaller yet observable ones. Certainly, had this not been true, large irregular crystals should have been observed.

B. Solvent Trapping Results

The crystallization growth velocities which we obtained were seen to be in the lower range of Myerson's[2] studies. As mentioned above, attempts to increase the growth rates were not entirely successful. At our growth rates Myerson observed from 3 to 12% excess water by weight (See Figure 16.) We found little or no trapping in the potassium alum crystals grown at these velocities in the suspension crystallizer.

Initially we examined all the sizes of a crystal sample for trapping. We later only baked the crystals above 30 mesh, thinking that small amounts of occlusions in the larger crystals were being masked by the larger total sample weight. Still we found no conclusive evidence that solvent was trapped in these larger crystals.

Our efforts in this regard were somewhat hampered by the baked alum crystal residue itself. Once the twelve hydrated waters were driven off by baking for several hours at 220°C, the residue was detected to have a tendency to absorb water from the air. This phenomenon was evidenced

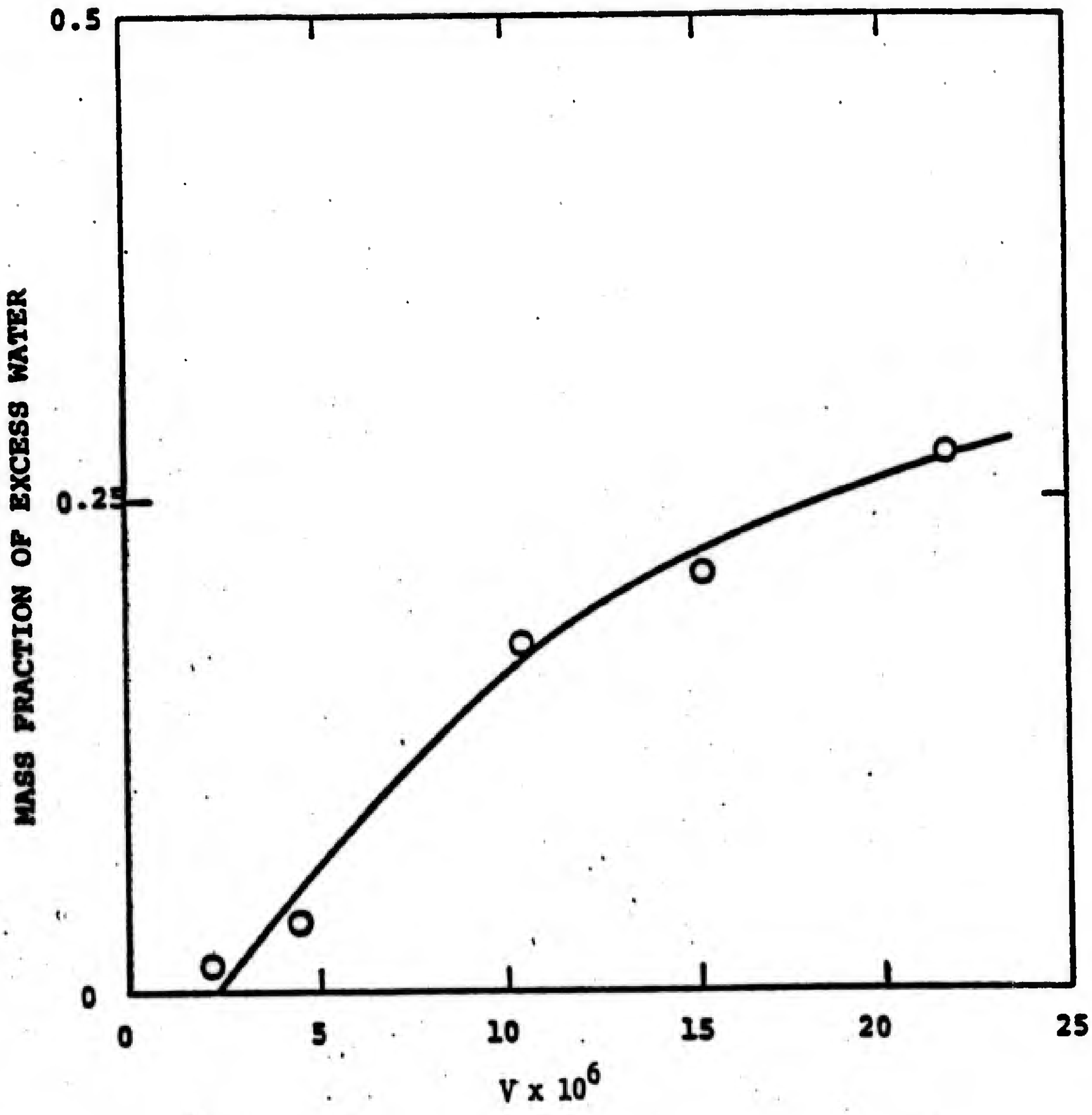

Figure 16. Effect of growth velocity on the amount of excess water in single $KAl(SO_4)_2 \cdot 12\ H_2O$ crystals grown from solution.

by a gain in weight while being weighed on the Mettler balance. Some studies were made, and a 1 gram sample of alum was seen to gain as much as 5% in weight after baking and exposure to the atmosphere. Cooling in a dessicator was found to be ineffective since the alum was generally more hygroscopic than the dessicant. Of course, had we been able to achieve larger growth velocities, the above effect would have been less of an experimental headache, since a greater fraction of solvent is predicted to be trapped.

Additionally, some criticism of this technique for measuring occluded solvent has been raised in the literature. The studies of Wilcox[5] and Denbigh and White[4] suggest that heating crystals above the boiling point of the trapped solvent is generally not enough to remove the occlusions. Wilcox[5] proposed that gradient techniques, either in temperature, pressure, or other means to create a chemical potential gradient across the crystal is the preferred method. The main argument against baking off the solvent is that it does not create a path for the solvent to escape. Rather the liquid may vaporize and still remain trapped within the crystal.

This argument is not felt applicable to the potassium alum system. As low as 64.5°C, 9 waters of hydration are known to be lost. As these and the remaining 3 waters boil, the crystals have been observed to "dissolve" in these waters of hydration. A distinct physical change occurs wherein the crystals become molten and resolidify after all the water has been evaporated. Since the crystal structure has been broken by this dissolution in the waters of hydration, any additional, occluded water will certainly have an escape route. Therefore, the procedure used, as outlined above, is a viable technique in this system, but may not be the best for others.

In order to elucidate the phenomena governing the trapping of solution during growth, it would be well to compare the conditions under which potassium alum crystals were grown inthe experiments of Myerson and those of this study. Some of the factors which could be of importance are growth rate, mass transfer influences, crystal size, and particle-particle or particle-surface interactions.

As previously mentioned, the growth rates in the suspension crystallizer were generally lower than those of Myerson,[2] although there was some overlap in the region where he found trapping. Still larger growth rates could not be obtained in our cooling crystallizer because greater supersaturations were not attainable. Attempts to further increase our supersaturation resulted in crystallization on the cooling coil which soon prevented even the maintenance of the existing supersaturation. Increased heat transfer surface per unit volume would be required to achieve greater supersaturations. Related to this is the fact that both nucleation and growth compete for the existing supersaturation. Therefore, a reduction in the nucleation rate would probably be necessary to allow higher supersaturations. The not-well-understood nucleation rate is very difficult to control but would probably require drastic changes in the materials of construction and design of the crystallizer and agitator. It should be pointed out that these experiments were conducted under conditions of supersaturation and growth velocity which were generally higher than those reported in the past for continuous cooling crystallizers.[25] It is perhaps likely that the growth velocity per se is not the primary reason for the reduction in trapping, since the velocities where Myerson[2] observed trapping were attained.

Myerson's single crystal experiments were conducted in order to minimize mass transfer effects so that the growth rates were very nearly those obtained from the interfacial crystallization kinetics at the applied supersaturations. Similarly, as shown in the analysis leading to the results in Table 5, mass transfer influences were not large in the suspension crystallizer either, except at the lowest growth rates and saturations. Thus, it appears that individual crystals were growing primarily under kinetic control in both studies.

Myerson[2] grew alum seed crystals in the range of 0.148 - 0.206 cm in diameter to a size range of 0.32 to 0.4 cm. in diameter. The largest crystals grown in the continuous crystallizer were less than 0.2 cm. in diameter. This suggests that the difference in the size of the crystals in these two studies is significant to trapping. Brice and Bruton[39] theoretically suggest that, below a certain size, crystal faces <u>must</u> grow stably. This is essentially because there is only one two-dimensional nucleus, or step source, on the face. If one estimates the critical size of a face for potassium alum using their theory values in the range of .05 - .10 cm. are predicted. From this it appears that a minimum critical size may be necessary for a growing crystal to trap solution. Crystal size in the suspension crystallizer is governed essentially by nucleation rate. If fewer nuclei are produced, larger-sized crystals can grow from the existing supersaturation.

In a similar study Denbigh and White[4] reported that they could not find regular occlusion patterns growing hexamine crystals from aqueous solutions in a continuous crystallizer system operating at steady-state. However, these occlusions could be produced in a batch system. Furthermore, they found that the regular occlusions which formed in the batch system could not be detected at high (230 rpm) stirrer speeds. The stirring motor used in our study operated at about 1700 rpm. They found that increased speed produced secondary nuclei and hence, reduced the growth velocity per unit area of crystal, and produced more, but smaller crystals. Their final conclusion on the formation of crystal occlusions is that they tend to form above some critical size, and are not detected in smaller crystals.

Although it appears plausible that crystal size is very important to whether or not occlusion formation occurs, other possible effects, relevant to an agitated suspension crystallizer should be noted. Collisions of crystals with one another or with the walls of the vessel might cause dentritic-like projections to be continuously broken off, thus preventing subsequent entrapment of solution. Collisions may also cause crystal size to remain below a critical value due to fracturing larger crystals into smaller ones.

In order to test the hypothesis that crystal size is important to the phenomena of trapping, a need for single crystal studies analogous to those conducted by Myerson over a range of crystal sizes and growth velocities is indicated. Further work in suspension crystallization would also be valuable in elucidating the importance of size providing that the nucleation rate can be controlled.

Suspension crystallization of additional chemical systems is also indicated to demonstrate the generality of the conclusions thus far developed.

CHAPTER V

CONCLUSIONS AND RECOMMENDATIONS

1. An experimental CMSMPR crystallizer has been constructed and was shown to produce crystal size distributions from which growth velocities could be determined.
2. These growth velocities in the continuous suspension crystallizer are of the same magnitude of those for alum crystals as observed in single crystal growth studies.
3. The theory may be inadequate in determining the actual kinetics of the system due to breakage and secondary nucleation effects. Additionally, a size dependent model may be required.
4. No observable trapped solvent was detected probably due to the fact that larger crystals could not be produced.

In continuation of this study and to further investigate the results of other investigators, the following are recommended:

1. Improvement of our experimental design by the increase in heat transfer area per unit volume is needed to explore the effects of higher supersaturations than achieved in this study.

2. Suspension crystallization with subsequent occlusion analysis in additional chemical systems is needed to substantiate our conclusions for the potassium alum-water system.
3. The influence of size dependent growth should be investigated more fully for our system.
4. Additional comparisons between suspension crystallization and single crystal kinetics is needed for the development of trend analysis.
5. Additional experiments, both of single crystal and suspension growth, should be performed to determine if occlusions can form in small crystals or whether a certain minimum "critical size" must first be achieved.

LITERATURE CITED

1. Edie, D. D., "Impurity Capture in Crystallization," Ph.D. Dissertation, University of Virginia (1975).

2. Myerson, A. S., "Impurity Trapping During Crystal Growth," Ph.D. Dissertation, University of Virginia (1977).

3. Brooks, R., Horton, A. T., and Torgeson, J. L., *J. Cryst. Growth* *2*, 279 (1968).

4. Denbigh, K. G. and White, E. T., *Chem. Eng. Sci*. *21*, 739 (1966).

5. Wilcox, W. R., *Ind. Eng. Chem*. *60*, 13 (1968).

6. Edie, D. D. and Kirwan, D. J., *I. & E.C. Fund*. *12*, 100 (1973).

7. Cheng, C. T. and Pigford, R. L., *I. & E.C. Fund*. *10*, 220 (1971).

8. Kirwan, D. J. and Pigford, R. L., *A.I.Ch.E.J.* *15*, 442 (1969).

9. Janzow, E. F. and Chao, B. T., *Desalination* *12*, 141 (1973).

10. Ozüm, B. and Kirwan, D. J., *A.I.Ch.E. Symp. Ser*. *153*, 1 (1976).

11. Chernov, A. A., "Growth of Crystals," N. Sheftal ed., Vol. 3, 35.

12. Hall, R. N., *J. Phys. Chem*. *57*, 836 (1953).

13. Botsaris, G. D., Mason, E. A., and Reid, R. C., *A.I.Ch.E.J.* *13*, 764 (1967).

14. Reid, R. C. et al., *Ind. Eng. Chem*. *62*, 57 (1970).

15. Wilcox, W. R., *J. Appl. Phys*. *35*, 636 (1963).

16. Rutter, J. W. and Chalmers, B., *Can. J. Physics* *31*, 15 (1953).

17. Walton, D., Tiller, W. A., Rutter, J. W., and Winegard,

W. C., A.I.M.E. Trans. 203, 1023 (1955).

18. Tiller, W. A. and Rutter, J. W., Can. J. Phys. 34, 96 (1956).

19. Plaskett, T. S. and Winegard, W. C., Can. J. Phys. 37, 1555 (1959).

20. Cheng, et al., A.I.Ch.E.J. 13, 739 (1967).

21. Chalmers, B., et al., Acta. Met. 1, 428 (1953).

22. Mullins, W. W. and Sekerka, R. F., J. Appl. Phys. 34, 323 (1963).

23. Mullins, W. W. and Sekerka, R. F., J. Appl. Phys. 35 444 (1964).

24. Randolph. A. D. and Larson, M. A., A.I. Ch.E.J. 8, 639 (1962).

25. Randolph, A. D. and Larson, M. A., "Theory of Particulate Process," Academic Press, Inc., New York (1971).

26. McCabe, W. L., Ind. Eng. Chem. 21, 121 (1929).

27. Murray, D. C. and Larson, M. A., A.I.Ch.E.J. 11, 728 (1965).

28. Koros, W. J., Dalrymple, D. A., Kuhlman, R. P. and Brockmeir, N. F., A.I.Ch.E.J. Symp. Ser. 68, 67 (1972).

29. Randolph, A. D. and Rajagopal, K., I. & E.C. Fund 9, 165 (1970).

30. McCabe, W. L. and Smith, J. C., "Unit Operations of Chemical Engineering," McGraw-Hill, Inc., U.S.A. (1976).

31. Jones, A. G. and Mullin, J. W., Trans Instn. Chem. Engrs. 51, 302 (1973).

32. Jancic, S. and Garside, J., Chem. Eng. Sci. 30, 1299 (1975).

33. Mullin, J. W., Garside, J., and Unakabhokha, R., J. Appl. Chem. 15, 502 (1965).

34. Mullin, J. W. and Garside, J. Trans. Instn. Chem. Engrs. 45 T291 (1967).

35. Garside, J. and Jancic, S. J., A.I.Ch.E.J. 22, 887 (1976).

36. Perry, R. H. and Chilton, C. H., eds., "Chemical Engineers' Handbook," Mc-Graw Hill Book Company, New York (1973).

37. Botsaris, G. D. and Denk, E. D., I. & E.C. Fund. 9, 276 (1970).

38. Mullin, J. W. and Garside, J., Trans. Instn. Chem. Engrs. 45, T285 (1967).

39. Brice, J. C. and Bruton, T. M., J. Cryst. Growth 26, 59 (1974).

APPENDIX A

PHYSICAL PROPERTIES AND SOLUBILITY OF POTASSIUM ALUMINUM SULPHATE

Table 6

Physical Properties of Potassium Aluminum Sulphate

Formula	(gm/cc)	M.W.	Diffusivity (cm.^{2}/sec.) at 30°C	$k_a = 3.46$	$k_v = 0.471$
$KAl(SO_4)_2 \cdot 12\ H_2O$	1.757	474.39	5.03×10^{-6}		

Densities of Saturated Solutions

T(°C)	ρ gm./ml. soln.
15	1.047
20	1.054
25	1.062
27	1.066
30	1.072
40	1.098
50	1.142

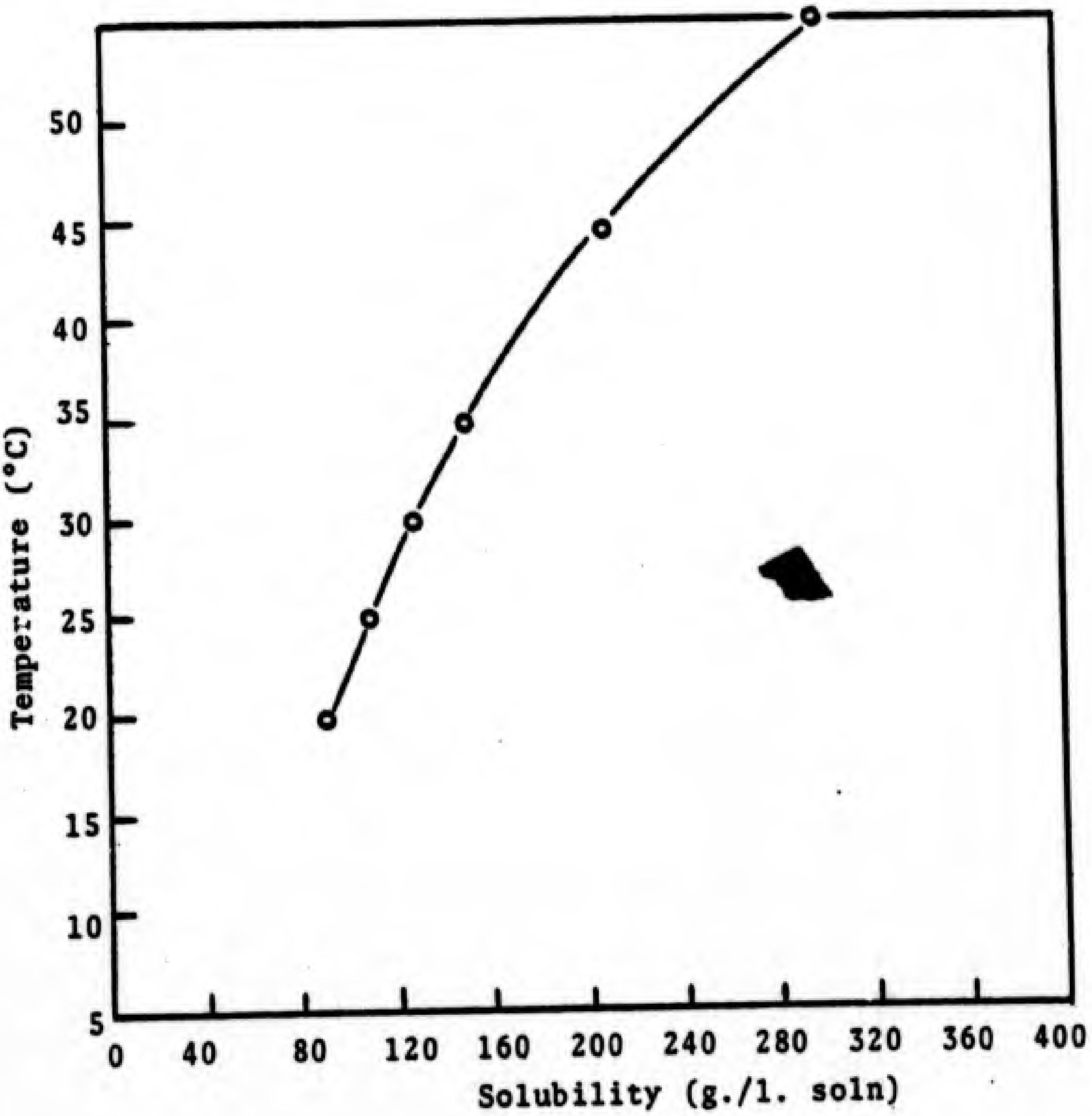

Figure 17. Solubility of potassium alum in water.

APPENDIX B

EXPERIMENTAL DATA AND OPERATING CONDITIONS

Table 7

Experimental Data and Operating Conditions*

Run #	Sample #	Feed T,°C	Crystallizer T,°C	Sample wt. gm./l. slurry	$V \times 10^6$ cm./sec.	τ sec
2	1	33.0	29.8	7.9677	4.84	2400
2	2	33.0	29.8	7.8404	5.14	2400
6	1	42.0	27.6	56.6683	4.01	3542
6	2	42.0	28.3	57.7821	3.93	3542
6	3	42.0	39.6	49.9529	3.99	3542
7	1	42.0	27.1	53.9935	7.25	1759
7	2	42.0	27.2	60.8282	8.07	1759
7	3	42.0	27.2	66.8653	7.94	1759
7	4	42.0	28.5	49.2390	7.58	1759
8	1	36.0	30.0	22.9023	4.86	2372
8	2	36.0	30.1	18.0994	4.74	2372
9	1	34.8	30.0	12.2622	4.52	2372
9	2	35.0	30.0	11.6910	5.09	2372
9	3	35.0	30.1	11.7602	4.80	2372
5	1	42.0	26.9	74.4446	1.60	10624
5	2	42.0	27.0	39.4224	1.26	10625
5	3	42.0	27.0	59.2048	1.39	10625
5	4	42.0	27.0	105.2866	1.28	10625

*The measured weight distributions are filed in the author's laboratory notebook.

APPENDIX C

U.S. STANDARD SCREEN DIMENSIONS

Table 8

U.S. Standard Screen Dimensions

Mesh Range	ΔL µm	$\bar{L}$ µm
-8 + 10	360	2180
-10 + 16	820	1590
-16 + 20	330	1015
-20 + 30	250	725
-30 + 40	175	512.5
-40 + 60	175	337.5
-60 + 80	70	215
-80 + 100	30	165
-100 + 140	44	128
-140 + 200	31	90.5